(NASA-CR-159979) A STUDY OF PARTICLE ACCELERATION MECHANISMS AND DYNAMICS OF THE OUTER TRAPPING REGION BY OBSERVATIONS AT SYNCHRONOUS ORBIT: A SUMMARY OF SCIENTIFIC RESULTS (Minnesota Univ.) 69 p

N80-24915

Unclas

G3/46 22051

A STUDY OF PARTICLE ACCELERATION MECHANISMS AND THE DYNAMICS OF THE OUTER TRAPPING REGION BY OBSERVATIONS AT SYNCHRONOUS ORBIT; A SUMMARY OF SCIENTIFIC RESULTS

Prepared By

K. N. Erickson

School of Physics and Astronomy

University of Minnesota

Minneapolis, Minnesota 55455

Cosmic Physics Technical Report No. 184

February, 1980

This document constitutes the final report for work done under contracts NAS 5-11687 (development) and NAS 5-23703 (analysis), J. R. Winckler, Principal Investigator.

TABLE OF CONTENTS

I. Introduction:

The University of Minnesota ATS-6 synchronous orbit satellite program was carried out as part of the continuing effort of Professor John Winckler and his group to study the origin and dynamics of energetic electrons and protons observed in the outer zone of stable trapping and in the near earth plasma sheet regions of the magnetosphere. Because of its location, the geostationary orbit (6.6 R_E) is well-suited for such studies. During times of magnetic disturbance this region is characterized by large and often rapid changes in the directional intensity of charged particles. The acceleration, dispersion, and loss processes which govern the population and motion of these particles in the local magnetic and electric fields depends on the energy, charge and pitch angle of the particles.

The energetic particles (>30 keV) measured by the University of Minnesota electron-proton spectrometer are sensitive indicators of substorm growth and expansion phase activity. Consequently, the data has been of great help in furthering our understanding of topics, such as; electrojet current characteristics, large scale auroral features, particle boundary motions, changes in the magnetosphere configuration associated with large scale current systems, and the effects of potential and inductive electric fields during these characteristic substorm phases. To extend the usefulness of our own experimental results we have correlated the observed particle intensity changes with other measurements, such as; local B, low energy particles, world-wide ground magnetometer data, local and ionospheric electric fields, interplanetary field, and plasma sheet data.

The ATS-6 instrument represented on extension of the type of spectrometer onboard ATS-1 and consisted of two nearly identical detector assemblies. Each of these assemblies was a magnetic spectrometer with three solid state electron detectors and one solid state proton detector. For each system electrons and protons were separately measured in three energy channels. The electron channels were approximately 30-50 keV, 150-215 keV, and greater than 500 keV. Protons were measured in channels of 30-60 keV, 60-160 keV, and 160-500 keV. One of the detector assemblies faced the spacecraft east direction and remained fixed. The other assembly mounted on a supporting post was rotated by a stepping motor so that the spectrometer scanned a range of spatial directions covering 180° from spacecraft north to south through west, remaining for 8 seconds at each of 13 positions separated by 15° steps. The major development of this spectrometer was carried out as a Master of Science thesis by Mr. James Wolf during the period 1970-74. A complete description of the instrument is contained in the thesis (Wolf, 1972) and in a technical report (Winckler, 1973). A description of the instrument has been published by Walker et al. (1975).

The directional capabilities of the scanning system together with the measured local magnetic field from the UCLA onboard magnetometer allowed the particle pitch angles to be calculated and studied. In addition, when the scanning system and fixed system were directed diametrically opposite it was possible to examine the spatial flux gradients in the radial direction and distinguish between a region of particles sweeping over the spacecraft and an intrinsic time variation. This capability to evaluate the guiding center particle density gradients has been of great use in our substorm related studies and in our study of magnetopause motions over the position of the ATS-6 satellite which occurred on September 15, 1974.

For protons the energy ranges selected covered the predominant proton population in the outer zone. The lower energy range included the protons which comprise a significant portion of the extraterrestrial ring current and which account for most of the particle energy density. These data have been of particular value in distinguishing true diamagnetic effects from the affects of distant currents. Electron channels cover the high-energy tail of plasma sheet electrons injected during substorms and is similar to the range of energies responsible for ionospheric absorption and auroral x-rays.

The relatively "narrow band" energy windows have provided better defined energies for observing the dispersion effects of drifting particles. Also, the sampling rates of 8/second for the lowest energy channels and 1/second for the higher channels has made possible the study of rapidly varying flux changes, including; changes due to rapidly moving boundaries, wave disturbances, and rapidly varying fluxes similar to those commonly observed in precipitated fluxes.

II. Research Completed and Scientific Results:

In this section we summarize briefly the principal scientific results obtained from our studies of the ATS-6 electron-proton spectrometer data. Further details may be found in the published papers and abstracts as referenced. For the sake of completeness and for convenient reference, the abstracts of all ATS-6 published and contributed or invited papers have been provided as Appendixes I, II, and III of this report.

Proton flux increases:

As discussed by Erickson et al. (1975) the substorm associated flux increases of energetic (E>30 keV) protons observed at 6.6 R_E may be grouped into four categories as follows:

1. Rapid flux increases associated with the motion of energetic particle boundaries.

2. Spectrum softening increases.

3. Spectrum hardening increases which do not exhibit energy dispersion.

4. Spectrum hardening increases which do exhibit energy dispersion.

Local time distributions for events in these groups as selected from a complete scan of a representative period during 1974 are shown in Figure 1. In sharp contrast to the energetic (E>30 keV) electron increases for which the energy spectrum softens and which are frequently observed post-midnight, the spectrum softening proton increases are only observed pre-midnight and then only relatively infrequently. In fact, such proton increases are observed only about 10% as frequently as the spectrum hardening ones. Utilizing adiabatic theory and a model which includes the sudden enhancement of a uniform cross-magnetosphere electric field and a model time-independent magentic field, the directional intensity increases of energetic protons observed at synchronous orbit has been qualitatively described (Walker and Erickson, 1975). In particular, the observed spectrum hardening of proton increases and the observed local time dependence of the changes in the proton pitch angle distribution, with increases near midnight occurring predominantly at large pitch angles and those observed near dusk occurring primarily at small pitch angles has been reproduced by the model. However, the observed energy dispersion as a function of pitch angle cannot be described by such a simple model as further discussed below in the third section.

Energetic particle intensity decrease-increase sequence and substorm morphology:

The rapid proton intensity increases observed on the nightside at synchronous orbit (e.g. boundary motion events of Figure 1) are always directly preceded by a decrease of from one-half to one hour in duration. This substorm associated sequence is a common feature of both the energetic proton and electron observations in the region near 6.6 R_E. We have found that this well-defined decrease-increase particle intensity sequence observed at synchronous orbit provides a clear temporal reference for the study of many other substorm signatures, which to date have included:

1. The B-field (UCLA magnetometer) at 6.6 R_E, especially the H-component which senses the cross-tail current and partial ring current in the outer magnetosphere. This provides a measure of the degree of tailward tilt of the magnetic field and consequently of the large-scale dynamic configuration changes of the nightside magentosphere.

2. The ground-based low- and mid-latitude H-component of the magnetic field which senses distant horizontal currents in the outer magnetosphere.

3. The ground-based H-component of the magnetic field (equivalently the AE index) at auroral latitudes which senses the intensity of the east-west oriented electrojet currents in the ionosphere.

4. The energetic (E>30 keV) particle density gradients at 6.6 R_E which provide a measure of the radial motion of these particle populations.

5. The low energy (0<E<30 keV) plasma (UCSD instrument) at 6.6 R_E. A knowledge of the behavior of the entire particle spectrum is important for understanding the relative affects of potential and inductive E-fields and the role they play in the convection, energization and acceleration of particles in the plasma sheet and synchronous orbit region. These low energy data also establish when injections of plasma sheet particles occur and/or when the ATS satellite is in the earthward part of the plasma sheet itself.

6. The very high energy (E>1.0 meV) electrons (Aerospace instrument) which establishes whether these relativistic particles are also affected, and if so in what way, by the substorm related processes.

7. The large-scale auroral arc structures. This provides insight into the temporal development of auroral structures in relation to electrojet intensification and the development of substorms as observed at synchronous orbit.

By means of this approach of utilizing the energetic particle decrease-increase sequence as a temporal reference we have been able to better organize and more fully understand the difficult and contraversial problem of the temporal development of magnetopsheric substorms. From these studies we have concluded that the energetic particle intensity <u>decrease</u> observed at synchronous orbit develops during the time period directly prior to substorm expansion phase onset. This time period has been referred to as the "growth" or "precursor" phase of the magnetospheric substorm. The energetic particle intensity <u>increase</u> which directly follows the decrease is clearly a signature of substorm expansion. Simply stated, the energetic particle intensity decrease-increase sequence at synchronous orbit corresponds identically to the "growth phase"-"expansion phase" sequence in the temporal development of the magnetospheric substorm and provides a clear temporal signature of these substorm phases.

Based on our studies we summarize the characteristics of the growth and expansion phases as follows:

1. Magnetic field at 6.6 R_E: During the growth phase, the H-component decreases (V-component increases at ATS-6) as the nightside magnetosphere develops into a more tail-like configuration. The total magnetic induction, B, may decrease or increase at ATS-6 depending upon the relative presence or absence of diamagnetic plasma. The expansion phase is characterized by an increase of the H-component to its previous level corresponding to a return of the inflated magnetosphere to a more dipole-like configuration. Figure 2 shows the H-component signature in terms of a super-posed epoch analysis using ATS-1 energetic electron data. The vertical dashed line would correspond to expansion phase onset. Further discussion may be found in Walker et al. (1976), Erickson et al. (1979) and Sauvaud and Winckler (1980). See also the example in Figure 3.

   It is important to stress that the decrease represents a distinct departure or "change of state" of the magnetosphere from its quiet time or average configuration state. The subsequent increase represents the return of the magnetosphere to its previous configuration state. Changes of state during the growth phase presumably involve the storage of additional energy in the more tail-like configuration of the magnetosphere. The subsequent release of this energy then occurs during the expansion phase. It is interesting that the range in size of magnetosphere distortion of "configuration states" observed for typical substorms falls within the extremes of diurnal distortion observed even on certain quiet days (see Erickson et al., 1979 for examples). Therefore, it should not be necessary to invoke any different mechanisms other than cha ges in large scale-current systems, such as, magnetopause or tail-currents to interpret the substorm associated configuration changes of the magnetosphere.

2. Tail-currents: The cross-tail current and its earthward part, the partial ring current intensify and/or move inward towards the earth during the growth phase which causes the distortion of the magnetosphere to a more tail-like configuration. At expansion phase onset an interruption and subsequent diversion of these currents occurs resulting in a return of the geo-

magnetic field to a more dipolar configuration (Erickson et al., 1979; Sauvaud and Winckler, 1980).

As discussed by Sauvaud and Winckler (1980) the tail-like distortion of the magnetic field during the growth phase cannot be alternatively described in terms of the diamagnetic effect of protons injected to synchronous orbit. However, an enhancement of the convection electric field in the tail would be consistent with the increase of the tail current system since it would at the same time increase the energy density of the charge carriers in the tail region of the magnetosphere and cause their movement toward the earth. Enhanced convection during the growth phase would increase the partial ring current outside 6.6 R_E and account for the major local time asymmetry in decrease events observed mostly in the evening sector by ATS-1 (Erickson et al., 1979).

3. Mid-latitude magnetic field (H-component): While the energetic particle intensity increase is clearly coincident with the onset of the H-component positive bays at mid- and low-latitudes the particle intensity decrease is not. Figure 4 (lower) indicates the results of a statistical timing study of the start of energetic particle intensity decreases and increases observed at ATS-1 and ATS-6 relative to the start of positive bays at mid-latitude (Erickson et al., 1979; Walker et al., 1977). This result provides strong evidence that the particle intensity decrease and subsequent recovery correspond to distinctly different substorm phases. The mid- and low-latitude H-components, which sense distant currents and which increase sharply coincident with the particle intensity increase indicate directly the interruption of the cross-tail current system at expansion phase onset. The observation that the H-component increases both at synchronous orbit and on the earth's surface places the tail-current systems outside of 6.6 R_E.

4. Auroral electrojet currents: Although electrojet currents intensity during the growth phase as well as the expansion phase, the intensification associated with expansion phase onset is generally much more pronounced and sharper. This is undoubtedly related to the rapid interruption and diversion of the tail current system, via field aligned currents, into the ionosphere at expansion phase onset. But even during the growth phase the electrojet currents are observed to intensify, often to large values, indicative of strong coupling between the electrojets and currents in the outer magnetosphere prior to expansion onset as well. Figure 4 (upper) shows the results of the timing study between the start of energetic particle intensity decreases and increases and the start of electrojet intensification. Specific examples of timing correlations may be found in the papers of Erickson et al. (1979) and Sauvaud and Winckler (1980). Electrojet current signatures, although they tend to be somewhat variable during the particle and H-component decrease

(growth phase), typically intensify in conjunction with the buildup and or inward motion of the tail current system. At expansion onset when the particles and H-component recover the electrojets rapidly further intensify above these pre-existing levels. These results are shown in the average sense by means of the super-posed epoch analysis of Figure 2. Here the AE index has been used as a measure of strength of electrojet currents and the vertical dashed line corresponds to particle recovery (expansion onset). Figure 3 also shows these results.

5. Energetic particles (E>30 keV): The synchronous orbit decrease of particle intensity which is coincident with the decrease of the magnetic field H-component (Figures 2 and 3 are caused by a shift of the trapped particle trajectories closer to the Earth on the night side following contours of constant B (Sauvaud and Winckler, 1980). Guiding center particle density gradients indicating the earthward (inward) motion during the growth phase and tailward (outward) motion during the expansion phase of energetic particles have been directly measured (Walker et al., 1976; Sauvaud and Winckler, 1980). As they circulate around the Earth these energetic particles are under the control of the gradient and curvature of the magnetic field. When the field inflates to a more tail-like configuration the particles must move inward. And this results in a decrease of particle intensity at the ATS satellite because of the decreasing radial flux profile with distance. When the field returns to a more dipolar configuration the particles must move outward resulting in a recovery of the particle intensity at the satellite.

During the growth phase as the particle intensity decreases the pitch angle distributions at synchronous orbit change from pancake (maximum at 90^{o}) to butterfly (minimum at 90^{o}) (Sauvaud and Winckler, 1980). The expansion phase restores the pancake type distributions.

Another clear expansion phase feature is the injection and acceleration of particles into synchronous orbit on the nightside. These injections extend to energies greater than 30 keV, particularly for electrons, and for these higher energies are caused by an induced electric field due to the change of B to more dipolar. This induced field would act in the same sense as the convection electric field which may also be enhanced at expansion phase onset (Erickson et al., 1979; Sauvaud and Winckler, 1980). Figure 3 shows two examples of the injection toward the Earth of additional fluxes (i.e. above the level present before the prior decrease) of 32-51 keV electrons. It is important to note that for particles of higher energy the fluxes just return to previous levels (the fluxes of electrons with energy greater than 50 keV, not show, have a behavior identical to the protons in Figure 3). As noted above, the fluxes of these more energetic particles are primarily modulated in response to the return of B to more dipolar as the particles move outward away from the Earth. This behavior is particularly characteristic of very energetic particles whose trajectories are not altered by electric fields. The critical energy separating particles injected to ATS orbit earthward from the tail and particles which move outward from the Earth to ATS orbit can be a function of time and of the location of the satellite relative to injection boundaries and the region affected by the changes in magnetic field topology. Walker et al. (1976) have experimentally shown both these kinds of movements are observed for particles of about 60 keV.

6. Low energy plasma ($0 \leq E \leq 30$ keV): It is well-established that the injection of plasma sheet particles to the synchronous orbit is coincident with substorm expansion phase onset. These injections correspond to the sudden invasion of the trapping zone by plasma from the tail region caused by an enhancement of the dawn-dusk convection electric field and/or the addition of an inductive electric field. During the growth phase the behavior of the lower energy plasma observed at synchronous orbit tends to be quite variable. As the more energetic particle intensity decreases, the lower energy plasma may increase (although always much less pronounced than at expansion phase onset), may decrease or not change. The particular signature observed will depend upon the strength of the convection electric field relative to the inductive field (now acting in the opposite sense) which results from the change of B to a more tail-like orientation. The ATS-6 satellite has also been observed to intercept the inner edge of the plasma sheet during the time of the growth phase (Sauvaud and Winckler, 1980).

7. Very high energy particles ($E > 1.0$ MeV): The relativistic particles at synchronous orbit respond to the substorm-associated dynamic charges of the magnetic field in the same way as the energetic particles discussed above. These particle intensities also decrease during the growth phase and recover at expansion phase onset (Sauvaud and Winckler, 1980). Observations of these relativistic particles strongly supports the picture of movement of the energetic particle populations first inward towards the Earth (particle decrease-growth phase) and then outward towards the tail (particle increase-expansion phase) in accord with the modification of the topology of the magnetic induction.

8. Auroral features: As first discussed by Erickson and Winckler (1979) there exists a close temporal correlation between the large-scale auroral features and the energetic particle intensity changes at synchronous orbit. Figure 5 illustrates

this close temporal relationship for two successive decrease-increase events on 1-2 February, 1968. Shown is all-sky camera data from Fort Yukon and College, the AE index, and energetic electron and magnetic field data, from ATS-1. Coincident with the particle decrease a quiet East-West arc system appears then intensifies and moves equatorward as the decrease and more tail-like orientation (as shown by the decreasing H-component) of the magnetic field develops. This is seen to be the case prior to each of the expansion phase onsets as indicated by the auroral breakup about 2244 and 0127. The intensification of the arc system prior to breakup indicates enhanced precipitation of auroral particles. If the enhancement of these lower energy precipitated fluxes is due to instabilities near the inner edge of the plasma sheet, the equatorward motion of the arc system is consistent with the motion of the plasma sheet earthward during the growth phase. We have found that during some decreases, "pseudo-breakup" activity, such as, surges or loops may appear in the aurora. However, these features appear and fade on a time scale of just a few minutes as the particle intensity at synchronous orbit continues to decrease. The major auroral "breakup" which occurs at the subsequent expansion phase onset always coincides closely with the particle intensity and magnetic field recovery and with additional intensification of the electrojet currents (see Figure 5).

In Figure 6 is shown an example of a particle flux decrease - increase sequence for comparison with auroral features obtained by the DMSP satellite 8531. The format of the data is the same as before and was obtained by ATS-6, located at 94°W longitude, on 5-6 November, 1974. The particle flux and H-component traces, again follow each other closely. The vertical line at 2221 ATS-6 local time corresponds to the time when the DMSP satellite tracking from north to south crossed the equatorward edge of the arc structure. At this time the track of the DMSP satellite was 20° eastward of ATS-6. The auroral feature at this point of the decrease is seen to be a double homogeneous arc structure which extends across the evening and midnight sector. In contrast, the next orbit of 8531, 100 minutes later, clearly shows active break-up auroral features. The time at which the DMSP satellite crossed the equatorward boundary of the auroral features corresponds to 0008 ATS-6 local time as indicated by the vertical line. This time corresponds to particle flux and H-component recoveries and a strong AE signature typical of substorm expansion. At this time the track of the DMSP satellite was at the same longitude as ATS-6.

<u>Energy and pitch angle dispersion of protons</u>:

The paper by Walker et al. (1978) reports the results of a study of the energy and pitch angle dispersion of energetic (E > 27 keV) proton flux enhancements observed at ATS-6 orbit. The observed energy dispersion of these substorm-associated proton flux enhancements corresponds to the highest energy protons arriving first as the particles drift westward to the ATS-6 position. Such energy dispersion has generally been interpreted as evidence that these particles have gradient- and curvature-drifted to the spacecraft from an injection region near midnight. In our study, the time of arrival delays observed between different proton channels were found to be smaller than those predicted by a simple model of drift in a dipole magnetic field. The use of more sophisticated field models and the inclusion of a cross-magnetosphere electric field improved the fit to the observed delays somewhat, but in all cases the observed delays were less than those predicted by the models.

Since the particle drift velocity in a dipole magnetic field is a maximum at 90^o pitch angle, the drifting proton enhancements should also exhibit dispersion in pitch angle with the 90^o pitch angle particles arriving first at the satellite. In the evening quadrant, proton enhancements at 90^o pitch angle arrived at the spacecraft prior to those at small pitch angles, as would be expected for particles drifting in a dipole-like magnetic field. However, on the dayside the increase occurs first at the smallest pitch angle ($\sim 30^o$). The difference between the arrival times of the 30^o and 90^o protons increases for more westward local time.

These observations place severe restrictions on the simple drift models and we have suggested that since the particle drift velocity is a field geometric quantity, a modification of present magnetospheric magnetic field models for the region near synchronous orbit is required.

Pitch-angle anisotropy:

Using the energetic particle pitch angle data from the University of Minnesota ATS-6 experiment Kaye et al. (1978) have reported large equatorial diurnal variation in pitch angle anisotropy. On the dayside during times of high $|B|$ it was observed that J (α=90^{o}) > J (α=40^{o}). In contrast during times of low $|B|$ on the nightside it was observed that J (α=40^{o}) > J (α=90^{o}). The results of a study of the observed particle anisotropies in terms of adiabatic and cyclotron resonance theory indicated that adiabatic effects are the dominant modulation mechanism of particle pitch angle distributions in the outer radiation belt.

Pc 4-5 energetic particle oscillations:

Erickson et al. (1978) have reported on a study of 80-270 second period proton flux oscillations at synchronous orbit. Figure 7 shows an example of an oscillation event observed at ATS-6 on 24 September, 1974. The panel on the right is an amplified and expanded plot of the data between the vertical dashed lines shown on the left panel. Of the 65 events studied in detail, 26 events (40%) are of the type shown in Figure 7. This type, observed near the dawn meridian, is characterized by having all proton channels in phase while the proton fluxes oscillate generally out of phase with the electrons and with the magnetic field components. There are two other predominant types observed: the first, observed at all local times, where the protons of different energy channels oscillate successively out of phase and the second, observed predominantly near dusk, where all proton channels show oscillations in phase and where the proton fluxes oscillate in phase with the electrons and with the V-component of the magnetic field.

A scan of seven months of E > 35 keV proton data from the ATS-6 experiment provided 165 oscillation events of at least 15 minute duration. The local time distribution of these events is shown in Figure 8 where the shaded distribution represents a subset where all three proton channels exhibited oscillations and which corresponds to the events we have studied in more detail. Figure 8 shows that the occurrence distribution of events in local time contains two distinct broad peaks having approximately equal numbers of events centered at 0600 LT near dawn and at 1600 LT near dusk.

Of the 65 proton oscillation events studied in more detail, 85% have accompanying oscillations of the local magnetic field. The magnetic signature of the dawn events indicates azimuthally polarized waves while the waves near dusk are radially polarized. All events seem to be left elliptically polarized. In terms of wave period and polarization the events having accompanying magnetic oscillations may be grouped into three classes: the 100-150 second dawn azimuthal class; the 100-150 second dusk radial class; the 200-250 second afternoon compressional class.

The proton oscillation events (15%) for which there is no evidence of local magnetic field fluctuations do not occur at any particular local time and may occur near a null region or node of the magnetic field line oscillation.

Comparison studies between energetic particle intensity charges at ATS-6 and auroral x-ray and optical emissions:

Results of correlative studies between ATS-6 energetic particle data and auroral x-ray and optical emissions have been reported by Parks and Lin (1975), Kaye et al. (1975), Gurgiolo et al. (1975) and Parks (1977).

The prinicpal findings of these studies are summarized as follows:

1. Intense auroral x-rays are detected in the region conjugate to ATS-6 when trapped electron fluxes undergo large non-adiabatic increases. The correlation is excellent for events that occur between midnight and noon. When ATS-6 was positioned at 94°W longitude the correlation with auroral x-rays was sometimes found to be more complicated than the close correlations which have been observed with the electron fluxes measured on ATS-1 at 150°W longitude. This is because ATS-6 was then on a higher L-shell and frequently in the plasma sheet. Consequently, the balloons flown near the foot of the nominal ATS-6 field line and the satellite were not always on the same magnetic lines of force. When ATS-6 was in the trapped radiation regions, the balloon, and the ATS-6 energetic particle data were found to be well-correlated, confirming the previous ATS-1 results.

2. The adiabatic particle flux increases observed at ATS-6 (94°W longitude) in the evening magnetosphere at the time of expansion phase onset are correlated with intense precipitation near Kiruna (35°E longitude), indicating the entire magnetosphere takes part in the dynamic substorm process.

3. Flux oscillations of the ATS-6, 32-51 keV trapped electron data in the 10 second period range have been found to correlate with over 50% of 20-50 keV Bremsstrahlung x-ray oscillation events having spectral peaks in the 10 second range. The x-ray oscilla-tion events are observed most frequently during 0600-0800 LT. These correlations suggest that wave-particle interactions operate on these energetic electrons.

4. Periodic 10 second variations detected in balloon borne H_β photometric data during a substorm event on August 18, 1974, have been correlated with similar oscillations in the 27-51 keV proton data from ATS-6. The presence of 10-second period oscillations were also observed in the synchronous orbit data. However, the proton variations occurred about two minutes before the H_β variations.

III. Research in Progress

The University of Minnesota electron-proton spectrometer experiment onboard ATS-6 has provided an extensive data set of energetic particle measurements at synchronous orbit. These data, when used in conjunction with data from the EME experiments and with other world-wide measurements, will continue to be of great value for the study of a wide variety of magnetospheric phenomena. In our ongoing studies of the ATS-6 data we are currently working on three topics as described briefly below.

1. <u>The energetic particle intensity decrease-increase sequence at synchronous orbit: A temporal reference for the study of magnetospheric substorms</u>: Using the particle decrease (growth phase signature) - increase (expansion phase signature) sequence at synchronous orbit as a temporal reference we are extending the substorm studies discussed in Section II. This work includes: additional correlative studies of the large scale auroral features utilizing all-sky and DMSP images; a study of the particle precipitation features using riometer and DMSP data; correlative studies of the IMF signatures; an investigation of plasma sheet particle and field signatures; a study of the low- and mid-latitude H-component signature just prior to the positive bay; and a more extensive study of the magnetic field components both on the ground and at synchronous orbit, particularly the east-west component which is most directly related to field-aligned currents.

2. <u>Pc 4-5 oscillations of energetic particle fluxes at synchronous orbit</u>: In addition to the work discussed in Section II, we are, in cooperation with the UCLA group, performing additional work to better classify and interpret the observed Pc 4-5 particle modulations. We are working to statistically establish the characteristics of proton oscillations for which there are no significant field oscillations and in the reverse sense the pattern of field oscillations, if any, for which there are no particle oscillations. Also being completed is a more extensive correlation of the proton oscillations with the electron data and an additional spectral and coherency analysis of the waves to determine polarization, ellipticity, etc. for all of the 165 selected events.

3. <u>Magnetopause crossings by the ATS-6 satellite on 15, September, 1974</u>: On this day during the interval 1345-1815 UT (0730-1200 ATS-6 local time) the magnetopause was on several occasions

observed to move back and forth past the position of the ATS-6 satellite. Using the ATS-6 magnetic field data (UCLA experiment) we are determining the magnetopause normal for each crossing by the method of minimum variance and by the cross-product method. Magnetopause orientations so determined, during these times when the magnetopause is moved inward to 6.6 R_E, are compared with the average or model magnetopause orientation. The energetic particle boundaries at the magnetopause are being studied in relation to the magnetopause configuration specified by the magnetic field signatures. By transforming to a coordinate system where one axis is selected to lie along the magnetopause normal, it is possible, knowing the time rate of change of B for the two components in the plane of the magnetopause and the velocity of magnetopause motion (v_{mp}), to determine the current density vector (J) in the plane of the magnetopause. The rate of change of B can be found directly from the transformed data and v_{mp} can be determined by studying the motion of the particle boundaries obtained from the particle density gradients. In this way J can be directly determined. Knowing the magnetic field signature, and J and having information on the particle trajectories from the particle density gradient measurements we will be able to study existing models of magnetopause current systems. We are also studying the nature of the magnetic field rotations during the crossings to determine whether the discontinuity is rotational or tangential in nature which would be associated respectively with an open magnetosphere or closed magnetosphere.

IV. Engineering Performance

As noted previously, the University of Minnesota experiment onboard ATS-6 has provided a large amount of excellent data on energetic particles at synchronous orbit. In addition to providing measurements on particle gradients, the redundancy of having two independent spectrometers proved itself to be very valuable. The scanning system performed particularly well, with all detectors providing over 12 months of continuous data. Despite many difficulties during the development stage with the scan drive system, it performed magnificently in orbit for more than 19 months of continuous operation. The problem areas of detector noise and premature failure of the proton and >500 keV electron detectors are discussed below.

The detectors used in the electron-proton spectrometer were obtained from the Ortec Corporation and are gold-silicon surface barrier type with a sensitive depth of 300 μm (except for the proton detector which is 200 μm) and have either 25 or 50 mm^2 sensitive area. They are reversed biased to about 100 V and have a noise width of between 6 and 9 keV full width at half maximum (FWHM) at room temperature. In the spectrometer the detectors are fitted into ports which are closed tightly by an iron cover to complete the magnet yoke. The detectors are operated with the aluminum face receiving the particles and the gold junction facing away to reduce radiation damage.

The experiment has 12 output counting channels furnishing a standardized logic pulse for each particle recorded in the three proton and electron energy windows of each spectrometer. The 12 channels and a summary of detector performance is given in Table 1.

TABLE 1 DETECTOR OPERATION SUMMARY

System	Energy Range (keV)	Detector Status	Date	Amount of Good Data (months)
Scanning System+				
Electrons	32-51	Functional	as of 2/15/76	>20
	150-214	Functional	as of 2/15/76	>20
		Noise Problem		
		2200-0300 UT	2/12/75-6/01/75	
		1330-1700 UT	3/26/75-6/01/75	
		1500-1900 UT*	6/01/75-	
		0600-0900 UT*	6/01/75-	
	>500	Failed	6/19/75	12
Protons	27-51	Failed	6/19/75	12
		Noise Problem		
		1800-2200 UT	10/01/74-6/19/75	
	51-120	Failed	6/19/75	12
	120-377	Failed	6/19/75	12
Fixed System				
Electrons	32-44	Functional	as of 2/15/76	>20
		Noise Problem		
		1800-2200 UT	7/27/74-4/01/75	
		1330-2400 UT	4/01/75-6/01/75	
		0600-1600 UT*	6/01/75-	
	150-211	Failed at launch	6/14/74	—
	>500	Failed	2/06/75	8
Protons	35-63	Failed	2/06/75	8
		Noise Problem		
		1700-2100 UT	8/01/74-2/06/75	8
	63-160	Failed	2/06/75	8
	160-514	Failed	2/06/75	8

+The mechanical drive for the scanning system failed ~ 1/30/76 after more than 19 months of continuous trouble-free operation.

*ATS-6 at 35°E longitude location. Since the observed noise problems are ATS-6 local time dependent, the UT time of noise occurrence shifts accordingly. ATS-6 local midnight is ~0615 UT at 94°W and ~ 1450 UT at 35°E.

The energy edges of the various windows are defined as the point at which the count rate response due to a discrete energy pulse drops to one-half its value in the center plateau of the energy window. As usual with gold-silicon particle counters, the detector and preamplifier input noise is added to the pulse charge deposited in the silicon diode by the incident particle and caused a spread in the observed pulse heights even from a beam of monoenergetic particles. Thus, the above definition is necessary. The input noise is a strong function of temperature. The detector system was designed to operate at about $0^{o}C$ (or colder) by means of passive radiation balance by coating the surface of the iron magnet with white paint with high solar diffuse reflectivity. The experiment package was designed to be fastened to the surface of the EME base structure with the two detectors protruding through the thermal blanket. As indicated in Table 1 enhanced noise problems became apparent in the lowest energy proton and electron channels in the course of the mission. This detector noise is ATS-6 local time dependent, occurring during the noon to dusk quadrant of the orbit, and appeared first in the fixed detector system. ATS-6 local noon for the $94^{o}W$ longitude position is 1815 UT. Any increase of temperature above room temperature would begin to introduce detector noise into the lowest energy proton or electron spectrometer channels. Because the temperature of the spectrometer is thus critical, each spectrometer head was equipped with a thermistor, and in addition a third thermistor was placed in the electronics package next to the base plate to monitor the EME support structure temperature. The diurnal variations in the temperatures was found to be more than 70^{o} which was far above the $0\text{-}24^{o}C$ variations specified to the experimenters for design purposes. The cause of the large temperature extremes is thought to be the reflecting or focusing of solar radiation from the thermal blanket covering the EME package to the spectrometer heads, thus increasing the radiative heat flux input. This problem was found during spacecraft tests in solar simulation prior to launch, but was not solved, so that in orbit the problem reappeared. The passive thermal control of the spectrometer heads was carefully measured and it was found that the combination of heat conduction through the support tube and the reflectance of the spectrometer coatings was capable of maintaining the temperature in a satisfactory range even in full sunlight in orbit. The high temperatures are encountered, however, when the solar radiation becomes normal to the thermal blanket covering the EME package. The higher than anticipated temperatures have caused the observed noise problems. It has been observed that the background counting rates during the high temperature part of the day at local noon increased as detector noise became high enough to enter the low-energy proton window. At local midnight the background counting rate remained relatively constant at 10 counts/s, corresponding to spectrometer head temperatures at about $-40^{\circ}C$. However, at 1300 local time during the high temperature region of the orbit, the background rate increased progressively to more than 1000 counts/s, indicating an unacceptable thermal noise background level. The effect of the high temperature has been more pronounced on the proton and electron detector in the fixed spectrometer and these detectors prematurely failed about 8 months after launch, as noted in Table 1. See also Walker et al. (1975).

The 150-200 keV channel in the fixed detector has given no data on the mission. The cause of this data outage has not been determined.

It is also important to note that, as shown in Table 1, the proton detectors and E > 500 keV electron detectors failed first. Protons entering the entrance collimator are directed against the proton detector and not deflected by the magnetic deflection system. Similarly, E > 500 keV electrons are also not appreciably deflected by the magnetic and directly strike the detector. These detectors which were exposed to direct bombardment of radiation failed first. This suggests radiation damage effects may have shortened detector lifetime.

While a great deal of information is available on radiation damage effects on solid state detectors for protons and electrons with energies above 1 meV, little information is available concerning low energy protons common to the ATS-6 experiment. The main reference which is applicable is a 1968 paper by Coleman, et al. (IEEE Transactions on Nuclear Science, 15, 482, 1968) in which the damages in silicon surface barrier detectors by 50 keV, 200 keV, 600 keV, and 1.00 meV protons are measured for fluences from 10^{10} to 10^{14} protons/cm^2. Current, noise, capacitance, and counting response to Am-241 alpha particles were measured as a function of reverse bias voltage. The detectors used by Coleman were manufactured by Ortec, Inc., as were the ATS-6 detectors.

Most of Coleman's measurements were made with the detector's gold contact as the entrance window. He concluded that above 10^{11} protons/cm^2, increase in leakage current due to proton damage appears to be directly proportional to fluence, and detector noise increases very rapidly above 10^{13} protons/cm^2. In order to compare these results to the ATS-6 detectors, we need some idea of the flux the ATS-6 detectors have been exposed to. An exact calculation would involve integrating data for each day of detector operation. To avoid this, we made use of a flux vs. energy plot for a "typical" day, using data from experimenters at the University of Minnesota, NOAA, and the University of California at San Diego. By simple graphical techniques the area under the curve was approximately 7.6 x 10^6/cm^2-sec-ster. Since the detector collimator has length L and area A, the spherical dependence can be removed by the geometric factor A/L^2 (5.1 x 10^{-3}ster). Considering ATS-6 active for 1 year, which corresponds to 3.15 x 10^7 seconds, we have, for a time interval of one year:

$$\text{flux} = (7.6 \times 10^6 \text{ cm}^{-2} \text{ sec}^{-1} \text{ ster}^{-1})\ (5.1 \times 10^{-3} \text{ ster}$$
$$(3.15 \times 10^7 \text{sec})$$
$$= 1.2 \times 10^{12} \text{ protons/cm}^2$$

Based on Coleman's results this amount of flux should not damage the bulk silicon enough to be responsible for the type of damage evident on ATS-6. If the ATS-6 detectors used the gold contact as the entrance window, it would not be unusual to find damage beginning to occur at 10^{12} protons/cm^2. However, using the aluminum contact as the entrance should boost the threshold for damage by a factor of 10^2-10^3. It is possible that a dead layer might be formed near the aluminum contact making efficient detection of low energy protons impossible. But this layer should not effect collection efficiency for higher energy protons; the ATS-6 detectors became inoperative for all proton energies.

One alternate explanation for the damage may be surface currents. Theoretical treatment of surface currents is not adequately understood and hence is not discussed in any pertinent reference. However, it appears that surface currents are the principal source of noise in surface barrier detectors. Coleman's work does not consider surface damage, but he remarks that surface damage may be important when considering low energy protons that are stopped near the detector surface. Since ATS-6 experiences a large flux of these low energy protons, it seems probable that surface damage may be an important factor to consider. Until more is known about surface currents, it is not possible to pinpoint the exact cause of the detector failures or to predict if altering parameters such as bias voltage or sensitive depth would result in detectors with longer lifetimes. All tests of the ATS-6 detectors were normally done without voltage bias on the detectors.

V. Data Processing:

Routine processing of most of the useable data has been completed and currently a large data set is readily accessible for study. To date over a year of continuous electron and proton data obtained when ATS-6 was located at 94°W longitude and three months of data from the 35°E location, has been processed. This data includes: 24-hour daily summary plots of 96-second averaged data, listings of 32-second averaged data on magnetic tape. High time resolution data has also been processed for our correlative studies on auroral zone x-ray events, for studies of particle boundary motions, proton oscillations and for studies of the inward motion of the magnetopause over the ATS-6 location on September 15, 1974. Data in the format of 24-hour daily summary plots from June 14, 1974 - March 31, 1975, has thus far been provided to the National Space Science Data Center (NSSDC). Additional data through August 31, 1975, will also be provided to NSSDC.

ACKNOWLEDGEMENT

The assistance of R. Swanson, V. Heinen, N. Larson, P. Durkee, B. Lundell, J. Steffen, K. Sougstad, L. Denninger and T. Hanson with the data processing, analysis and display is gratefully acknowledged. We also thank Professor Carl McIlwain for furnishing the lower energy ATS-6 particle data, Dr. George Paulikas for the very energetic ATS-1 particle data, and Professors McPherron and Coleman of UCLA for vector magnetic data from both ATS-1 and ATS-6. Magnetograms and other data have been supplied by the World Data Center A for Solar Terrestrial Physics and by the National Space Science Data Center.

The University of Minnesota ATS-6 program was supported by the National Aeronautics and Space Administration under contracts NAS 5-11687 (development) and NAS 5-23703 (analysis). Additional analysis support was provided under contract NSG-07005.

APPENDIX I

ABSTRACTS OF ATS-6 PUBLISHED PAPERS

WINCKLER GROUP

ATS-6 SYNCHRONOUS ORBIT TRAPPED RADIATION STUDIES WITH AN ELECTRON-PROTON SPECTROMETER

R.J. Walker, K.N. Erickson, R.L. Swanson, J.R. Winckler

School of Physics and Astronomy, University of Minnesota
Minneapolis, Minnesota 55455

ABSTRACT

The University of Minnesota Electron-Proton Spectrometer Experiment consists of two nearly identical detector assemblies. One of these assemblies was mounted in a position fixed on the satellite in the Environmental Measurements Experiments (EME) east direction and the other was rotated so that the spectrometer scanned a range of spatial directions covering 180° from EME north to EME south through west. Each of the detector assemblies is a magnetic spectrometer containing four gold-silicon surface barrier detectors. This instrument provides a very clean separation between protons and electrons by the combination of pulse height analysis and magnetic deflection. Each detector assembly measures protons in three nominal energy ranges (30-50 keV), (50-160 keV), and (120-514 keV). Electrons also are measured in three energy intervals (30-50 keV), (150-214 keV), and (more than 500 keV). Data are transmitted from the experiment at rates as high as 8 measurements/s. Decreases in the flux of the energetic electrons and protons followed by very rapid increases are frequently observed on the nightside during periods of geomagnetic activity. Separation of temporal and spatial effects is possible using proton gradient information obtained when the detector systems are oppositely directed. Using this technique, the decreases have been interpreted as motion of the trapping region equatorward and Earthward of the satellite. The boundary motion associated with the particle recovery shows a marked local time dependence. Particle increases observed in the evening sector have been interpreted as motion from Earthward and equatorward of Applications Technology Satellite-6 (ATS-6). Recoveries in the morning sector represent motion presumably of the near Earth plasma sheet from north and tailward of the spacecraft. In the region about midnight both types of motion are observed. Frequently the recovery from beneath the satellite is followed by motion tailward of ATS-6.

IEEE Trans. Aerosp. Electron Syst., 11, 1131-1137, 1975.

SUBSTORM-ASSOCIATED PARTICLE BOUNDARY MOTION AT SYNCHRONOUS ORBIT

R.J. Walker, K.N. Erickson, R.L. Swanson, J.R. Winckler

School of Physics and Astronomy, University of Minnesota
Minneapolis, Minnesota 55455

ABSTRACT

Decreases in the flux of energetic (>30 keV) electrons and protons followed by very rapid increases are characteristic of the magnetospheric substorms observed on ATS 6 at synchronous orbit in the region about midnight. By using proton gradient information from the University of Minnesota electron-proton spectrometer the decreases are interpreted as a physical motion of the trapped particle outer boundary from the satellite toward a region equatorward and earthward of the satellite. The particle recoveries are found to be associated with an expansion phase onset of a magnetospheric substorm. The motion corresponding to these flux increases may be organized into three types according to the direction of the gradient. In the most common type of recovery the flux increase is observed first on guiding centers north and tailward of the spacecraft and represents motion, presumably of the plasma sheet, from north and tailward to south and earthward of ATS 6. This motion is observed most frequently near local midnight. Recoveries are also observed over a broad local time range on the nightside, in which the indicated motion is from earthward and equatorward of the satellite to a region above and tailward. For other particle increases observed in the evening sector a recovery associated with motion from beneath the satellite to above the satellite frequently is followed by a second increase enveloping the satellite from north and tailward.

J. Geophys. Res., 81, 5541-5550, 1976.

PITCH ANGLE DISPERSION OF DRIFTING ENERGETIC PROTONS AT SYNCHRONOUS ORBIT

R.J. Walker, K.N. Erickson, J.R. Winckler

School of Physics and Astronomy, University of Minnesota
Minneapolis, Minnesota 55455

ABSTRACT

The time of arrival at ATS 6 of substorm-associated energetic (>27 keV) proton flux enhancements has been examined as a function of both energy and pitch angle by using data from the University of Minnesota electron-proton spectrometer. The protons exhibit energy dispersion with the particles with the highest energy arriving first. This energy dispersion generally has been interpreted as evidence that these particles have gradient- and curvature-drifted to the spacecraft from an acceleration region on the nightside. In the evening quadrant, proton enhancements at 90° pitch angle arrived at the spacecraft prior to those at small pitch angles, as would be expected for particles drifting in a dipolelike magnetic field. However, on the dayside the increase occurs first at the smallest pitch angle (~30°). The difference between the arrival times of the 30° and 90° protons increases for more westward local times. For the highest energy range observed (120-377 keV), drifting protons are rarely seen at large pitch angles. These observations place severe restrictions on the simple drift models. Since the pitch angle dependence of the particle drift velocity is a field geometric quantity, the observations require the modification of present magnetospheric magnetic field models. In particular, the models need to reproduce better the enhanced field observed on the dayside near synchronous orbit. The particle energy and pitch angle dispersion observations may provide a sensitive test of future models.

J. Geophys. Res., 83, 1595-1600, 1978.

ADIABATIC MODULATION OF EQUATORIAL PITCH ANGLE ANISOTROPY

S.M. Kaye, C.S. Lin, G.K. Parks

Space Sciences Division, Geophysics Program, University of Washington
Seattle, Washington 98195

J.R. Winckler

School of Physics and Astronomy, University of Minnesota
Minneapolis, Minnesota 55455

ABSTRACT

Particle measurements from the University of Minnesota detector aboard the geostationary ATS 6 satellite reveal striking equatorial pitch angle anisotropies. A study of 7 days of data shows a diurnal variation in anisotropy with $J(\alpha=40^{\circ}) > J(\alpha=90^{\circ})$ during times of low $|B|$ on the nightside and $J(\alpha=90^{\circ}) > J(\alpha=40^{\circ})$ during times of high $|B|$ on the dayside. Six representative anisotropy events are studied in finer detail. The 32- to 51-keV electron anisotropies increase and decrease with the total magnetic field intensity. The proton and higher energy electron anisotropies do not show as much variation. The particle anisotropies are studied in light of adiabatic and cyclotron resonance theory; the results indicate that adiabatic effects are the dominant modulation mechanism of particle pitch angle distributions in the outer radiation belt.

J. Geophys. Res., 83, 2675-2682, 1978.

A STUDY OF MAGNETOSPHERE DYNAMICS DURING AURORAL ELECTROJET EVENTS BY OBSERVATIONS OF ENERGETIC ELECTRON INTENSITY CHANGES AT SYNCHRONOUS ORBIT

K.N. Erickson, R.L. Swanson, R.J. Walker, J.R. Winckler

School of Physics and Astronomy, University of Minnesota
Minneapolis, Minnesota 55455

ABSTRACT

A statistical study of over 1600 events has established that a close temporal correlation exists between the start of energetic electron directional intensity changes observed at synchronous orbit and the intensification of electrojet currents in the polar ionosphere. This result provides strong evidence that both phenomena are physically linked as part of a large-scale disturbance and that the electrojet system is closely coupled to other current systems in the distant magnetosphere. The statistical pattern in local time of these electrojet-associated electron intensity variations consists of decreases observed in the pre-midnight sector, increases observed over a broad region symmetrical about midnight and spectrum softening increases observed post-midnight. In the local evening sector intensity decreases and increases are observed with equal probability and typically occur as two parts of a single time sequence such that the decrease directly precedes the increase. Furthermore, while the start times for the decrease and the subsequent increase are both well-correlated with a marked electrojet intensification the increase is also well-correlated with a mid-latitude positive bay but the decrease is not. This difference together with the fact that decreases systematically precede increases in the local time region where both are observed strongly suggests that the decrease corresponds to a distinct "precursor" of the increase event which follows. These results are important for understanding the temporal development of magnetospheric disturbances and are also not consistent with "the fault-line" concept which suggests that the pre-midnight decrease corresponds to a simultaneous increase event occurring further eastward in local time. The intensity decreases are closely correlated with a decrease in the local magnetic field and have been interpreted in terms of the electrons responding to a diamagnetic reconfiguration resulting from an enhancement of the particle energy density due to convection of plasma sheet protons into the pre-midnight region. The subsequent intensity increases are accompanied by an increase in the local magnetic field and can be associated with a tail-field collapse at expansion onset.

J. Geophys. Res., 84, 931-942, 1979.

DYNAMICS OF PLASMA, ENERGETIC PARTICLES, AND FIELDS NEAR SYNCHRONOUS ORBIT IN THE NIGHT TIME SECTOR DURING MAGNETOSPHERIC SUBSTORMS

J-A Sauvaud and J.R. Winckler

School of Physics and Astronomy, University of Minnesota
Minneapolis, Minnesota 55455

ABSTRACT

We discuss two phases of the substorm-associated magnetospheric dynamics in terms of the particles and fields at synchronous orbit. The first phase corresponds to the "decreases" of energetic particle flux first identified by Erickson and Winckler (1973) and discussed by Walker et al. (1976) and Erickson et al. (1979). This phase begins one-half to one hour before the substorm onset and is characterized by (1) a distortion of the magnetosphere to a more tail-like configuration caused by (2) an intensification and/or motion towards the Earth of the cross-tail current and of its Earthward part, the partial ring current, (3) a shift of trapped particle trajectories closer to the Earth on the night side following contours of constant B causing the particle "decreases"; accompanied by a change in the pitch angle distributions from "pancake" to "butterfly" as observed at geostationary orbit, (4) an initiation of a response of the AE index.

The decreases of energetic particle flux can correspond to the substorm growth phase as defined initially by McPherron (1970) or the growth or precursor phase of Erickson et al. (1979). Plasma motions and currents during decreases tend to be variable, but the description in paragraph one nevertheless characterizes the large-scale trend. It is suggested that the electric field induced by the increasing tail current near the Earth acts opposite to the cross-tail convection field and can temporarily inhibit convection near the geostationary orbit.

The second phase is the conventional expansion phase which begins with the "onset", characterized in our study by (1) a sudden decrease in the tail current and a return of the inflated magnetosphere to a dipole-like configuration, (2) a sudden shift of trapped high energy particles towards the tail again following contours of constant B and at the same time (3) a surge of tail plasma towards the Earth as the induced electric field now <u>increases</u> the total convection field. Separate effects thus result in the dramatic increases of both high energy and plasma particles seen at substorm expansion phase onset, (4) an AE index response and the appearance of bays at stations near midnight local time accompanied by very active aurora as well as the precipitation of high energy particles. The different appearance of the responses at the ATS-1 (on the magnetic equator) and the ATS-6 (off the magnetic equator) can be well explained by the above description. True diamagnetic effects of the particle population are clearly evident at the ATS-6 region, and must be carefully distinguished from the effects of distant currents. The use of oppositely directed detectors on ATS-6 which permits the evaluation of the guiding center particle density gradients has been of great use in this analysis.

In press, J. Geophys. Res., 1980.

APPENDIX II

ABSTRACTS OF ATS-6 CONTRIBUTED AND INVITED PAPERS

WINCKLER GROUP

SUBSTORM ASSOCIATED PARTICLE BOUNDARY MOTION AT SYNCHRONOUS ORBIT

R.J. Walker, K.N. Erickson, R.L. Swanson, J.R. Winckler

School of Physics and Astronomy, University of Minnesota

Minneapolis, Minnesota 55455

ABSTRACT

Decreases in the flux of energetic (>30 keV) electrons and protons followed by rapid flux increases are frequently observed during substorms by the University of Minnesota electron-proton spectrometer on ATS-6. These events are typically found within a few hours of local midnight. Using proton flux gradients, we have interpreted these events as particle boundary motion. The magnetic field magnitude measured by the UCLA magnetometer is anti-correlated with the particles indicating a strong diamagnetism. The energy density change of the measured particles is too small to account for the observed field change during the particle flux decrease but can account for the field change during the increase. All of the decreases are consistent with equatorward-earthward boundary motion. The velocity associated with this thinning motion range between 2 km/sec and 8 km/sec. Rapid oscillation of the boundary across the spacecraft are also frequently observed. The flux increases are usually associated with an outward expansion of the boundary from south of the spacecraft in the pre-midnight sector. In the post-midnight sector the increases frequently are associated with rapid inward boundary motion from north and tailward of the spacecraft. The velocities associated with rapid inward boundary motion from north and tailward of the spacecraft. The velocities associated with these increases range between 20 km/sec and 120 km/sec. This boundary, presumably the near earth boundary of the plasma sheet, exhibits a filamentary sturcture.

EOS Trans. AGU, 56, 422, 1975.

ATS-6 OBSERVATIONS OF AN UNUSUAL TRANSIENT CHANGE IN THE AMBIENT PARTICLE POPULATION PRECEDING A SUBSTORM

A. Konradi

Johnson Space Center, National Aeronautics and Space Administration
Houston, Texas 77058

T.A. Fritz

Space Environment Laboratory, National Oceanic and
Atmospheric Administration, Boulder, Colorado 80302

A.J. Masley

Aerojet ElectroSystems Co.
Azusa, California 91702

B.H. Mauk

Department of Physics, University of California at San Diego
La Jolla, California 92093

R.L. McPherron

Department of Planetary and Space Science, University of California
Los Angeles, California 90024

G.A. Paulikas

Space Physics Laboratory, The Aerospace Corporation
Los Angeles, California 90009

R.J. Walker

School of Physics and Astronomy, University of Minnesota
Minneapolis, Minnesota 55455

ABSTRACT

On 20 July 1974 at 0518 UT the complement of particle detectors and the magnetometer on ATS-6 observed an unusual pulse event at 2300 LT. The event occurred 35 minutes after one prompt substorm particle injection and preceded another substorm injection by about two minutes. The duration of the event was less than one minute. The characteristics of the event are a 10% increase in the northward component of the magnetic field and a complete temporary change in the spectrum of ambient

protons and electrons. There is a marked increase in the proton flux between 50 keV and 300 keV with a peak increase of a factor of 10 at about 200 keV. Below 50 keV the proton flux shows a strong decrease. The electrons show a similar behavior. The 32-44 keV electrons increase by about a factor of 30 while no increase is seen above 150 keV. Similarly, below 20 keV the electron flux decreases. The flux of 0.5 to 0.8 meV α particles also shows a strong increase. An analysis of azimuthal asymmetries in the proton flux at the onset of the event suggests that the increase is due to a flux gradient passing the satellite in the earthward and southward direction with a speed of about 40 km/sec.

EOS Trans. AGU, 56, 1047, 1975.

SUBSTORM ASSOCIATED PROTON FLUX INCREASES AT SYNCHRONOUS ORBIT

K.N. Erickson, R.L. Swanson, R.J. Walker, J.R. Winckler

School of Physics and Astronomy, University of Minnesota
Minneapolis, Minnesota 55455

ABSTRACT

Increases in the flux of energetic (>30 keV) protons are frequently observed during substorms by the University of Minnesota electron-proton spectrometer on ATS-6. The increases which are most frequently observed in the afternoon and evening region are characterized by a marked hardening of the energy spectrum. The protons exhibit local time dependent energy dispersion with the increases occurring simultaneously at all energies near midnight while the change in the more energetic protons occurs first at earlier local times. The change in the proton pitch angle distribution during these flux increases is strongly local time dependent. The increases observed in the pre-midnight region occur primarily at 90^{o} while the largest increase at local times nearer noon is at smaller pitch angles. In an accompanying paper, these observations will be interpreted in terms of particle drift subsequent to enhancement of a cross magnetosphere electric field. These events are in addition to the very rapid flux increases observed near midnight which are associated with diamagnetism. These very rapid flux increases have been previously interpreted as particle boundary motion using proton flux gradient information. There is one additional type of proton flux increase. These events, in which the proton spectrum softens, most frequently occur pre-midnight. Such events are observed only about 10% as frequently as the spectral hardening ones.

EOS Trans. AGU, 56, 1048, 1975

PROTON ACCELERATION AT SYNCHRONOUS ORBIT BY A CROSS MAGNETOSPHERE ELECTRIC FIELD

R.J. Walker and K.N. Erickson

School of Physics and Astronomy, University of Minnesota
Minneapolis, Minnesota 55455

ABSTRACT

The time variation of the flux of energetic protons arriving at synchronous orbit subsequent to a sudden enhancement of a uniform cross-magnetosphere electric field has been calculated using adiabatic theory and a model time-independent magnetic field. The initial (t=0) particle distribution was taken to be spatially uniform within the region from which particles are convected to a synchronous orbit in 1 hour. Both a power law distribution function and one derived from pre-substorm ATS-6 particle observations were employed. The trajectories of particles of energy W and pitch angle α observed at a given position at time t were followed backward in time to determine their initial (t=0) energies and pitch angles. Liouville's theorem was then invoked to predict the flux at the desired position and time. The model successfully reproduces many of the qualitative changes observed in the fluxes of >30 keV protons observed by the University of Minnesota electron-proton spectrometer on ATS-6. In particular, the predicted rapid proton flux increases in the dusk to midnight quadrant associated with hardening of the energy spectrum are observed. The observed local time dependence of the changes in the proton pitch angle distribution, with the increases observed near midnight occurring predominantly at large pitch angles and those observed before dusk occurring primarily at small pitch angles, is reproduced by the model.

EOS Trans. AGU, 56, 1048, 1975.

PITCH ANGLE DISPERSION OF DRIFTING ENERGETIC PROTONS AT SYNCHRONOUS ORBIT

R.J. Walker, K.N. Erickson, J.R. Winckler

School of Physics and Astronomy, University of Minnesota
Minneapolis, Minnesota 55455

ABSTRACT

The time of arrival at ATS-6 of 164 substorm associated energetic proton flux enhancements has been studied as a function of pitch angle and energy using data from the University of Minnesota electron-proton spectrometer. The protons exhibit energy dispersion with the highest energy particles arriving first. This energy dispersion generally has been interpreted as evidence that these particles have drifted to the spacecraft from an acceleration region on the nightside. Since the particle drift velocity is a maximum at 90° pitch angle, the flux enhancements of 90° pitch angle should be observed first on the dayside. However, this situation is rarely observed. In the morning and afternoon quadrants, proton enhancements at the smallest pitch angle (~30°) arrived at the spacecraft prior to those at 90° pitch angle. The difference between the arrival times of the 30° and 90° protons increases for more westward local times. This difference is consistently larger for (51-120 keV) protons than for (27-51 keV) protons. For the highest energy range (120-377 keV), drifting protons are rarely seen at large pitch angles.

EOS Trans. AGU, 58, 482, 1977.

ON THE ORIGIN OF HIGH-ENERGY ELECTRON PRECIPITATION IN THE LOCAL MORNING SECTOR OF THE AURORAL ZONE

G. Kremser and J.W. Munch

Max-Planck-Institut fur Aeronomie

3411 Katlenburg-Lindau, Germany

K.N. Erickson, R.J. Walker, J.R. Winckler

School of Physics and Astronomy, University of Minnesota

Minneapolis, Minnesota 55455

W. Riedler

Technical University Graz

Graz, Austria

ABSTRACT

Auroral X-ray measurements from balloon-borne instruments and particle flux data from the University of Minnesota electron-proton spectrometer onboard the geosynchronous satellite ATS-6 are used to investigate the sequence of magnetospheric processes that lead to electron precipitation in the morning sector. The observations yield evidence for the following sequence:

(1) Generation of intense fluxes of high-energy electrons, probably inside the Alfven-boundary;

(2) eastward drift of these electrons in the geomagnetic and geoelectric fields;

(3) precipitation of electrons that starts at the arrival of 50-70 keV drifting electrons, but also includes electrons with much high energies.

Possible mechanisms for the generation of the electron fluxes and for the electron precipitation are discussed.

EOS Trans. AGU, 58, 916, 1977.

ENERGETIC PARTICLE FLUX CHANGES AT SYNCHRONOUS ORBIT AND THE TEMPORAL MORPHOLOGY OF SUBSTORMS

R.J. Walker, K.N. Erickson, R.L. Swanson, J.R. Winckler

School of Physics and Astronomy, University of Minnesota
Minneapolis, Minnesota 55455

The pre- and near-midnight region is characterized by dramatic changes in the energetic particle population during magnetospheric substorms. Statistical studies of particle intensity changes from ATS-1 at 150°W longitude and from ATS-6 at 94°W longitude reveal important similarities and differences. The (>50 keV) electrons observed on ATS-1 and the (>32 keV) electrons and (> 27 keV) protons observed on ATS-6 are characterized by intensity decreases followed by more rapid intensity increases. The flux changes on ATS-1 are well correlated with the local magnetic field while the flux changes on ATS-6 are anti-correlated. This difference can be understood by noting that ATS-6 is 10° above the magnetic equator and ATS-1 and hence is near the trapping boundary. The ATS-6 observations are interpreted as particle boundary motion while the ATS-1 observations represent dynamic changes within the trapped particle population. The start of the increases at both spacecraft are well correlated with auroral zone negative bays and mid-latitude positive bays while the preceding decreases are less well correlated with auroral zone negative bays and show no correlation with mid-latitude positive bays. Thus the particle intensity decreases and recoveries represent the temporal signature of substorms at synchronous orbit. Clearly the intensity increases occur in conjunction with magnetospheric substorm expansion while the decreases, although correlated with electrojet intensification, apparently represent a distinct precursor event which does not show all the characteristics typical of substorm expansion.

EOS Trans. AGU, 58, 1212, 1977.

LOCAL TIME SIGNATURES OF 80-270 SECOND PERIOD PROTON FLUX OSCILLATIONS AT SYNCHRONOUS ORBIT

K.N. Erickson and J.R. Winckler

School of Physics and Astronomy, University of Minnesota
Minneapolis, Minnesota 55455

R.L. McPherron and R.J. Walker

Institue of Geophysics and Planetary Physics, UCLA
Los Angeles, California 90024

ABSTRACT

A scan of seven months of E > 35 keV proton data from our ATS-6 experiment has provided 160 oscillation events of at least 15 minute duration. For over 50 of the events all three proton channels (35-63 keV, 63-160 keV and 160-514 keV) showed measureable oscillations. Most events occur during times of active AE with over 75% observed when 3+<Kp<5. The occurrence distribution of events in local time (LT) contains two distinct broad peaks having approximately equal numbers of events centered at 0600 LT near dawn and at 1600 LT near dusk. Proton flux oscillation amplitudes correspond on the average to a factoral change of 1.2 independent of energy and LT, with simultaneous oscillations in the 32-44 keV electron flux typically of smaller amplitude. Statistically there exists no clear relationship between proton oscillation amplitude and pitch angle. Near dawn 80% of the events have all proton channel oscillations in phase, but 90°-180° out of phase with the associated oscillations in total B and each of the components, V, D, and H. Near dusk the phase relationships are more complicated with only 50% of the events having all proton channels in phase and with a less systematic phase relationship to the magnetic field components. Total B is 90°-180° out of phase for 80% of the events near dusk, but 60% of the events are now in phase with the oscillations in the V-component. Also near dusk the probability of observing associated oscillations of larger amplitude in total B and the V and H components is greater. The probability of observing proton waves of longer period is also greater near dusk.

EOS Trans. AGU, 59, 356, 1978.

PARTICLE FLUX DECREASE-INCREASE EVENTS AT SYNCHRONOUS ORBIT AND THE TEMPORAL SEQUENCE OF QUIET ARC-BREAKUP AURORA

K.N. Erickson and J.R. Winckler

School of Physics and Astronomy, University of Minnesota
Minneapolis, Minnesota 55455

ABSTRACT

Energetic particle flux increases observed on ATS satellites in the pre- and nearmidnight region are preceded by a flux decrease of a few minutes to over an hour duration. Such increases are well-correlated with all substorm expansion onset signatures. The preceding flux decrease, although correlated with an enhancement of the electrojet current system, is not correlated with other onset signatures. Using all-sky camera data from the region conjugate to the ATS satellite it has been established that the typical auroral feature present during the decrease is a stable quiet arc structure. The arc is often first observed coincident with the start of or during the decrease. Although the quiet arc structure may be interrupted briefly by a minor break-up and then reappear it typically persists until it is observed to momentarily fade, brighten and clearly break-up coincident with the particle flux increase. This sequence of events strongly supports the conclusion that the flux decrease and the enhancement of a quiet arc structure are both manisfestations of a "precursor" or "growth" period prior to substorm expansion onset.

During this time, additional energy storage results in a more tail like magnetic morphology on the night side as the tail current grows. Energetic trapped particles, because of their magnetic drift, move closer to the earth. Enhanced electric fields cause the inner edge of the plasma sheet to move closer to the earth and as a result the poleward boundary of electron precipitation moves to lower latitudes.

EOS Trans. AGU, 60, 917, 1979.

APPENDIX III

ABSTRACTS OF ATS-6 CONTRIBUTED AND INVITED PAPERS

PARKS GROUP

CORRELATION OF 5-40 SECOND PERIODIC BEHAVIOR BETWEEN ATS-6 TRAPPED ELECTRONS AND CONJUGATE AURORAL X-RAYS

Stanley M. Kaye, Chin S. Lin, George K. Parks

Space Sciences Division, Geophysics Program, University of Washington

Seattle, Washington 98195

ABSTRACT

Bremsstrahlung X-ray data of 20-50 keV from high altitude balloon flights in Thompson, Manitoba, Canada were analyzed for the presence of periodic phenomena in the 5-40 second range. Three time periods were selected for this study, 2400-0200 LT, 0300-0400 UT, and 0600-0800 UT for the days of March 29, 1975; April 8, 1975; and April 9, 1975. Fifteen power spectrums were performed, and the results show that of all the spectral peaks found in the 10 second range, most of them are found during 0600-0800 LT. In searching for correlations between X-ray spectra and equatorial electron flux oscillations, power spectrums were also performed on 1 second averages of 32-51 keV trapped electron data (α= 75-85^{o}) received from the geostationary ATS-6 satellite. Electron flux oscillations in the 10 second period range are also observed, with over one-half of the X-ray oscillation events correlating with electron flux variations of the same frequency. The results suggest that the wave-particle interaction operates on electrons of both large and small pitch angles.

EOS Trans. AGU, 56, 1047, 1975.

10-SECOND PERIODIC VARIATIONS IN H_β EMISSIONS AND THE ATS-6 PROTON FLUXES

Christopher Gurgiolo, Chin S. Lin, George K. Parks

Space Sciences Division, Geophysics Program, University of Washington
Seattle, Washington 98195

ABSTRACT

Extremely periodic 10-second variations were detected in balloon borne H_β photometric data during a substorm event detected on August 18, 1974. It is noteworthy to mention that observations of periodic variations in H_β are quite uncommon. We have searched for similar structures in the proton data (27-51 keV) of the University of Minnesota experiment on the ATS-6. Power spectral analysis using the maximum entropy technique indicates presence of 10-second period for the equatorial data as well. However, the proton variations occurred about 2 minutes before the H_β variations. The UCSD plasma data on the ATS-6 indicate that during the interval of time when the H_β variations were observed, the distributuion function was considerably structured, more so than before or after the interval of H_β periodic variations. The observed distribution indicates a thermal energy of about 5-10 keV and a density of about 0.3-0.5 cc^{-1}. The beta for the plasma is about 0.1-0.2. The observed proton distribution is not a Maxwellian. Although the mechanism responsible must yet be worked out, one possibility is that the 10-second periodicity is associated with the ion cyclotron instability process.

EOS Trans. AGU, 56, 1048, 1975.

PARTICLE SOURCE AND ACCELERATION DURING SUBSTORMS

George K. Parks and Chin S. Lin

Space Sciences Division, Geophysics Program, University of Washington
Seattle, Washington 98195

ABSTRACT

Detailed correlation studies of data obtained from x-ray detectors and photometers that were launched on balloons from Thompson, Manitoba, Canada indicate that the ATS-6 and the balloons are not always on the same magnetic lines of force because the ATS-6 is frequently in the plasma sheet. When the ATS-6 is in the trapped radiation regions, the balloon and the ATS-6 energetic particle data are extremely well correlated, confirming the previous results of x-rays and ATS-1 electron data. A detailed analysis was made of the well-correlated substorm event of August 18, 1974. Using the equatorial plasma data of UCSD, we have come to the following preliminary conclusions concerning particle sources and acceleration. For energies 0.5 to about 20 keV, electron fluxes along B are considerably enhanced during substorms as compared to the fluxes before substorms. For the large pitch-angle particles, however, fluxes below about 1 keV decrease during substorms while the fluxes increase above 1 keV. The proton behavior is different. We find that for all pitch-angles, proton fluxes above 3 keV are enhanced during substorms while the fluxes below about 3 keV remain nearly constant. These observations are consistent with the interpretation that the small pitch-angle electrons are accelerated elsewhere from the equatorial plane and the large pitch-angle electrons are locally accelerated. The behavior of protons is less clear and as yet the source is undetermined.

DOS Trans. AGU, 56, 1048, 1975.

EQUATORIAL PITCH ANGLE ANISOTROPY AND PARTICLE PRECIPITATION

Stanley M. Kaye and George K. Parks

Space Sciences Division, Geophysics Program, University of Washington

Seattle, Washington 98195

ABSTRACT

Auroral X-ray fluxes detected in balloon flights at Thompson, Manitoba, Canada during March and April 1975 were correlated with simultaneous measurements of equatorial electrons from the conjugate geostationary ATS-6 satellite to study particle precipitation. 20-40 keV X-ray flux was compared to 30-50 keV and 150-214 keV electron fluxes with α=30-90°, and to electrons with α=8-15° with energies 0.1-81 keV. In studying the first set of electron data, large pitch-angle anisotropies were seen at various times in the midnight, post-midnight, and early morning hours, lasting for periods of time between ten minutes and two hours. An event on March 29, 1975 was studied in detail, revealing steadily growing pitch-angle anisotropies; using the relation $A=1-J(\alpha=40°)/J(\alpha=90°)$, these anisotropies grew from A=-.11 to A=.78 in both energy channels, with the observed flux values exceeding the critical limit. The flux modulations in each energy channel were in phase, suggesting possible adiabatic causes of the anisotropy. Study of the "field-aligned" electrons show no increase in flux levels, nor is there any rise in the level of X-rays. This data will be used to quantatively obtain the relationship between electron pitch-angle anisotropy and electron precipitation.

EOS Trans. AGU, 56, 1047, 1975.

THE ATS-AURORAL ELECTRON PRECIPITATION STUDIES

G.K. Parks

Space Science Division, Geophysics Program, University of Washington

Seattle, Washington 98195

Correlation studies of auroral X-rays obtained in ~40 high-altitude balloon flights with equatorial ≳ 31 keV electrons over the pitch-angle range ~0°-90°, detected onboard the ATS-1 and 6, are providing important clues about the outer Van Allen electron acceleration and precipitation mechanisms:

1. The ATS-1 correlation series shows that intense auroral X-rays are detected when trapped electron fluxes undergo large non-adiabatic increases. The correlation is excellent for events that occur between midnight and noon.

2. The adiabatic modulation of trapped fluxes in the evening magnetosphere is correlated with intense precipitation in the opposite hemisphere near Kiruma, indicating the entire magnetosphere takes part in the dynamic substorm process.

3. The degree of correlation between X-rays and the equatorial electron fluxes depends on the longitude where the ATS-6 is located, as well as on the auroral latitude where the balloons are launched. Owing to the limited view angle of X-ray detectors as well as the finite disturbance scale of electron acceleration and precipitation regions, the correlation of ATS-6 is markedly better with Kiruna than with Thompson, Canada.

4. Electron fluxes near the loss cone have now been detected when intense auroral X-rays are detected. The correlation is good, as anticipated. However, the equatorial fluxes are two orders of magnitude smaller than is required to account for the observed X-ray intensity. There could be further acceleration of precipitating electrons in transit between the magnetosphere and the ionosphere where the X-rays are produced.

5. Rapid time structures such as microbursts have not yet been detected on the equatorial plane. The absence of such structures supports the view that microbursts might be generated locally, ≲ 4 R_e from the surface of the earth.

EOS Trans. AGU, 58, 1212, 1977.

COMPLETE BIBLIOGRAPHY OF PUBLICATIONS
UNDER THE UNIVERSITY OF MINNESOTA
ATS-6 SYNCHRONOUS ORBIT SATELLITE PROGRAM

First Publications Began 1972

(complete to January, 1980)

ATS-6 PUBLISHED PAPERS - WINCKLER GROUP

Walker, R.J., K.N. Erickson, R.L. Swanson and J.R. Winckler, Studies of the Trapped Radiation at Synchronous Orbit with the University of Minnesota ATS-6 Electron-Proton Spectrometer, IEEE Trans. Aerosp. Electron. Syst., AES-11(6), 1131, 1975.

Walker, R.J., K.N. Erickson, R.L. Swanson and J.R. Winckler, Substorm-Associated Particle Boundary Motion at Synchronous Orbit, J. Geophys. Res., 81, 5541, 1976.

Walker, R.J., K.N. Erickson, and J.R. Winckler, Pitch Angle Dispersion of Drifting Energetic Protons at Synchronous Orbit, J. Geophys. Res., 83, 1595, 1978.

Kaye, S.M., C.S. Lin, G.K. Parks, and J.R. Winckler, Adiabatic Modulation of Equatorial Pitch Angle Anisotropy, J. Geophys. Res., 83, 2675, 1978.

Erickson, K.N., R.L. Swanson, R.J. Walker, and J.R. Winckler, A Study of Magnetosphere Dynamics During Auroral Electrojet Events by Observations of Energetic Electron Intensity Changes at Synchronous Orbit, J. Geophys. Res., 84, 931, 1979.

Sauvaud, J.-A., and J.R. Winckler, Dynamics of Plasma, Energetic Particles, and Fields near Synchronous Orbit in the Night Time Sector During Magnetospheric Substorms, J.Geophys. Res., In Press, 1980.

ATS-6 TECHNICAL REPORTS AND THESES - WINCKLER GROUP

Wolf, J.L., An Electron-Proton Spectrometer for Studies of the Trapped Radiation, M.S. thesis, School of Physics and Astronomy, University of Minnesota, 1972.

Winckler, J.R., Final Project Report for Electron-Proton Spectrometer ATS-F, Cosmic Physics Technical Report #163, School of Physics and Astronomy, University of Minnesota, Minneapolis, Minnesota, 55455, May, 1973.

Erickson, K.N., R.J. Walker, and J.R. Winckler, The ATS-6 Electron-Proton Spectrometer Experiment: A Summary of Recent Scientific Results and Suggested Future Research, Cosmic Physics Technical Report #173, School of Physics and Astronomy, University of Minnesota, Minneapolis, Minnesota, 55455, July, 1977.

Fritz, T.A., C.W. Arthur, J.B. Blake, P.J. Coleman, Jr., J.P. Corrigan, W.D. Cummings, S.E. DeForest, K.N. Erickson, A. Konradi, W. Lennartsson, A.J. Masley, B.H. Mauk, C.E. McIlwain, R.L. McPherron, G.A. Paulikas, K.A. Pfitzer, D.L. Reasoner, P.R. Satterblom, S.Y. Su, R.J. Walker, E.C. Whipple, Jr., B. Wilken, and J.R. Winckler, Significant Initial Results from the Environmental Measurements Experiment on ATS-6, NASA Technical Paper, 1101, National Aeronautics and Space Administration, Washington, D.C., 20546, December, 1977.

ATS-6 CONTRIBUTED AND INVITED PAPERS - WINCKLER GROUP

Walker, R.J., K.N. Erickson, R.L. Swanson, and J.R. Winckler, Substorm Associated Particle Boundary Motion at Synchronous Orbit, EOS Trans., 56, 422, 1975.

Konradi, A., T.A. Fritz, A.J. Masley, B.H. Mauk, R.L. McPherron, G.A. Paulikas, and R.J. Walker, ATS-6 Observation of an Unusual Transient Change in the Ambient Particle Population Preceding a Substorm, EOS Trans., 56, 1047, 1975.

Erickson, K.N., R.L. Swanson, R.J. Walker, and J.R. Winckler, Substorm-Associated Proton Flux Increases at Synchronous Orbit, EOS Trans. 56, 1048, 1975.

Walker, R.J., and K.N. Erickson, Proton Acceleration at Synchronous Orbit by a Cross Magnetosphere Electric Field, EOS Trans., 56, 1048, 1975.

Parks, G.K., C.E. McIlwain, and J.R. Winckler, Correlated Observations Between ATS-6 Particle Experiments and Balloon Borne X-Ray and Photometric Emissions in 3914 Å and Hβ, Proceedings of IUGG Sixteenth General Assembly, Grenoble, September, 1975.

Walker, R.J., K.N. Erickson, and J.R. Winckler, Pitch Angle Dispersion of Drifting Energetic Protons at Synchronous Orbit, EOS Trans., 58, 482, 1977.

Kremser, G., J.W. Munch, K.N. Erickson, R.J. Walker, J.R. Winckler, and W. Riedler, On the Origin of High-Energy Electron Precipitation in the Local Morning Sector of the Auroral Zone, EOS Trans., 58, 916, 1977.

Walker, R.J., K.N. Erickson, R.L. Swanson, and J.R. Winckler, Energetic Particle Flux Changes at Synchronous Orbit and the Temporal Morphology of Substorms, EOS Trans., 58, 1212, 1977.

Erickson, K.N., J.R. Winckler, R.L. McPherron, and R.J. Walker, Local Time Signatures of 80-270 Second Period Proton Flux Oscillations at Synchronous Orbit, EOS Trans., 59, 356, 1978.

Erickson, K.N., and J.R. Winckler, Particle Flux Decrease-Increase Events at Synchronous Orbit and the Temporal Sequence of Quiet Arc-Breakup Aurora, EOS Trans., 60, 917, 1979.

ATS-6 CONTRIBUTED AND INVITED PAPERS - PARKS GROUP

Kaye, S.M., C.S. Lin and G.K. Parks, Correlation of 5-40 Second Periodic Behavior Between ATS-6 Trapped Electrons and Conjugate Auroral X-Rays, EOS Trans., 56, 1047, 1975.

Gurgiolo, C., C.S. Lin, G.K. Parks, Ten-Second Periodic Variations in Hβ Emissions and the ATS-6 Proton Fluxes, EOS Trans., 56, 1048, 1975.

Parks, G.K., and C.S. Lin, Particle Source and Acceleration During Substorms, EOS Trans., 56, 1048, 1975.

Kaye, S.M., and G.K. Parks, Equatorial Pitch Angle Anisotropy and Particle Precipitation, EOS Trans., 57, 307, 1976.

Parks, G.K., The ATS -- Auroral Electron Precipitation Studies, EOS Trans., 58, 1212, 1977.

FIGURE CAPTIONS

Figure 1

Frequency of occurrence distributions in ATS-6 local time of energetic proton flux increases as selected from a complete scan of a representative period during 1974.

Figure 2

161 superposed traces of AE index, 50-150 keV and 150-500 keV electron counts and magnetic induction in the 21^h-24^h MLT bin, selected from about 300 days of data with Kp $\leq 4^+$. The heavy line shows the superposed epoch average for all 161 events in this local time bin. The dots with dashed lines indicate the background curve, obtained by a superposition of all the 300, 24 hour-day intervals with Kp $\leq 4^+$. The start of each event (T=0) was chosen at the onset time of the 150-500 keV electron count increase (from Swanson, 1978). The entire 24 hour period is shown in the upper panel for the same T=0.

Figure 3

Example of the variations of the flux of energetic protons and electrons (32 second averages) and of the local magnetic induction B and its H component antiparallel to the terrestrial dipole axis recorded on 20 July, 1974, between 00^h and 10^h UT on board ATS-6. The corresponding AE index is also shown. ATS-6 local time (or MLT) is indicated at the top of the figure and UT at the bottom.

Figure 4

Number of events versus the time difference Δt, of ATS-1 and ATS-6 the energetic particle event start time minus the electrojet intensification start time (upper) and minus the start time of mid-latitude positive bays (lower). The number of events are indicated in parentheses.

Figure 5

Two successive energetic electron intensity decrease-increase sequences at ATS-1 on 1-2 February, 1968, for comparison with all-sky auroral images obtained at Fort Yukon and College. Also shown are the H-component at ATS-1 and the AE index. ATS-1 local time is indicated on the figure.

Figure 6

An energetic proton flux decrease-increase sequence at ATS-6 on 5-6 November, 1974, for comparison with DMSP images obtained on two successive passes of satellite 8531. Also shown are the H-component at ATS-6 and the AE index. ATS-6 local time is indicated on the figure. The dashed vertical lines indicate when the DMSP satellite tracking from north to south crossed the equatorward edge of the arc structure.

Figure 7

Example of an energetic particle oscillation event observed at ATS-6 on 24 September, 1974. Also shown are the VDH components and the total magnetic induction, B. The panel on the right is an amplified and expanded plot of the data between the vertical dashed lines shown on the left panel.

Figure 8

Frequency of occurrence distribution in ATS-6 local time of 165 proton oscillation events.

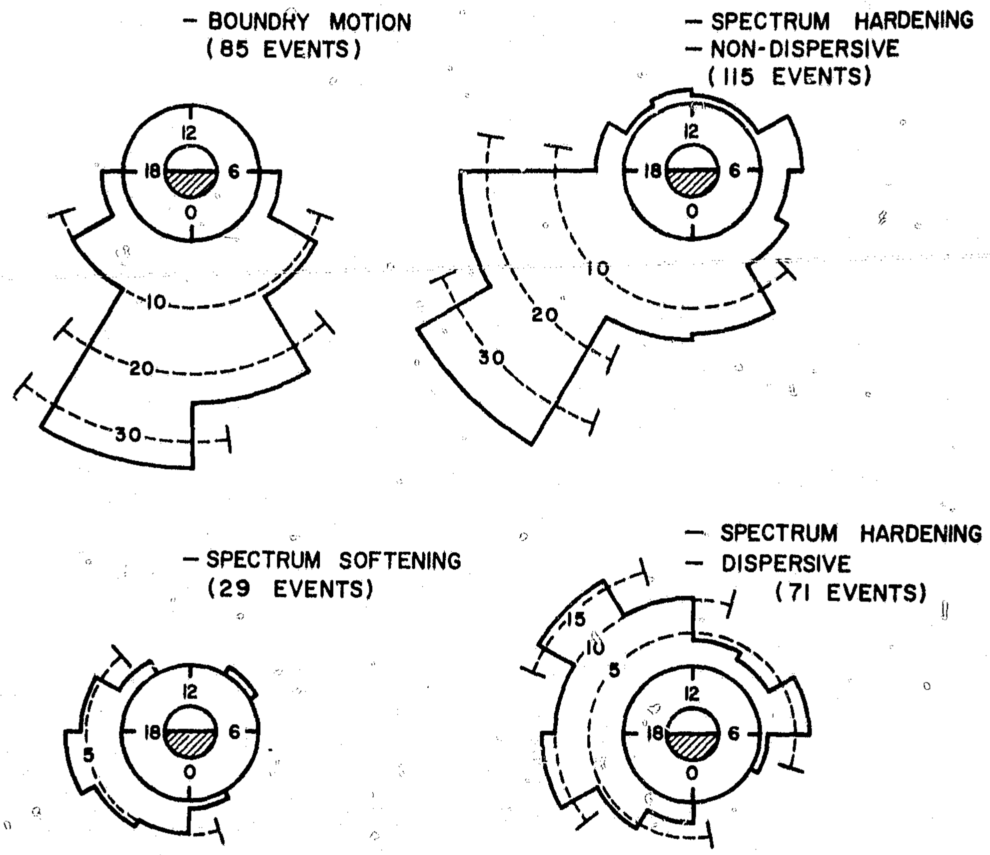
- BOUNDRY MOTION
(85 EVENTS)
- SPECTRUM HARDENING
- NON-DISPERSIVE
(115 EVENTS)
- SPECTRUM SOFTENING
(29 EVENTS)
- SPECTRUM HARDENING
- DISPERSIVE
(71 EVENTS)
12
18
6
0
10
20
30
5
15

FIGURE 1

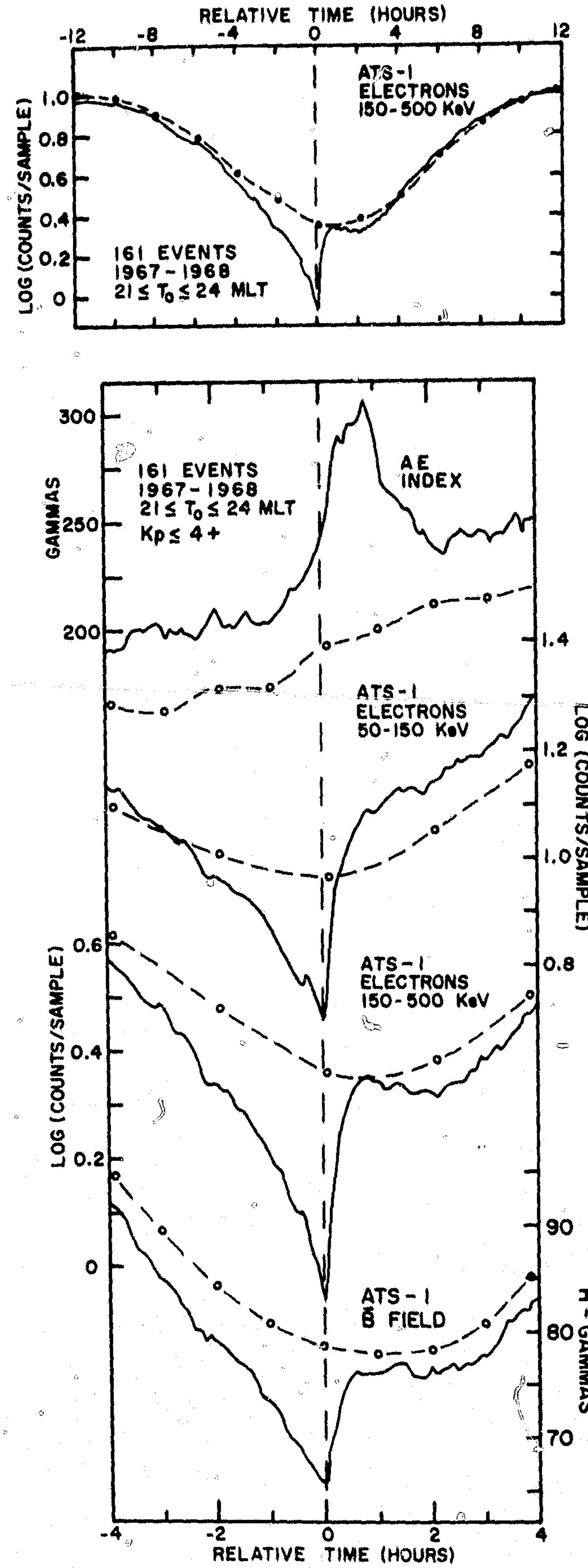

RELATIVE TIME (HOURS)
-12
-8
-4
0
4
8
12
ATS-1
ELECTRONS
150-500 KeV
LOG (COUNTS/SAMPLE)
1.0
0.8
0.6
0.4
0.2
0
161 EVENTS
1967-1968
21 ≤ T_0 ≤ 24 MLT
300
250
200
GAMMAS
161 EVENTS
1967-1968
21 ≤ T_0 ≤ 24 MLT
Kp ≤ 4+
AE
INDEX
ATS-1
ELECTRONS
50-150 KeV
1.4
1.2
1.0
0.8
LOG (COUNTS/SAMPLE)
ATS-1
ELECTRONS
150-500 KeV
0.6
0.4
0.2
0
LOG (COUNTS/SAMPLE)
ATS-1
$\vec{B}$ FIELD
90
80
70
H-GAMMAS
-4
-2
0
2
4
RELATIVE TIME (HOURS)

FIGURE 2

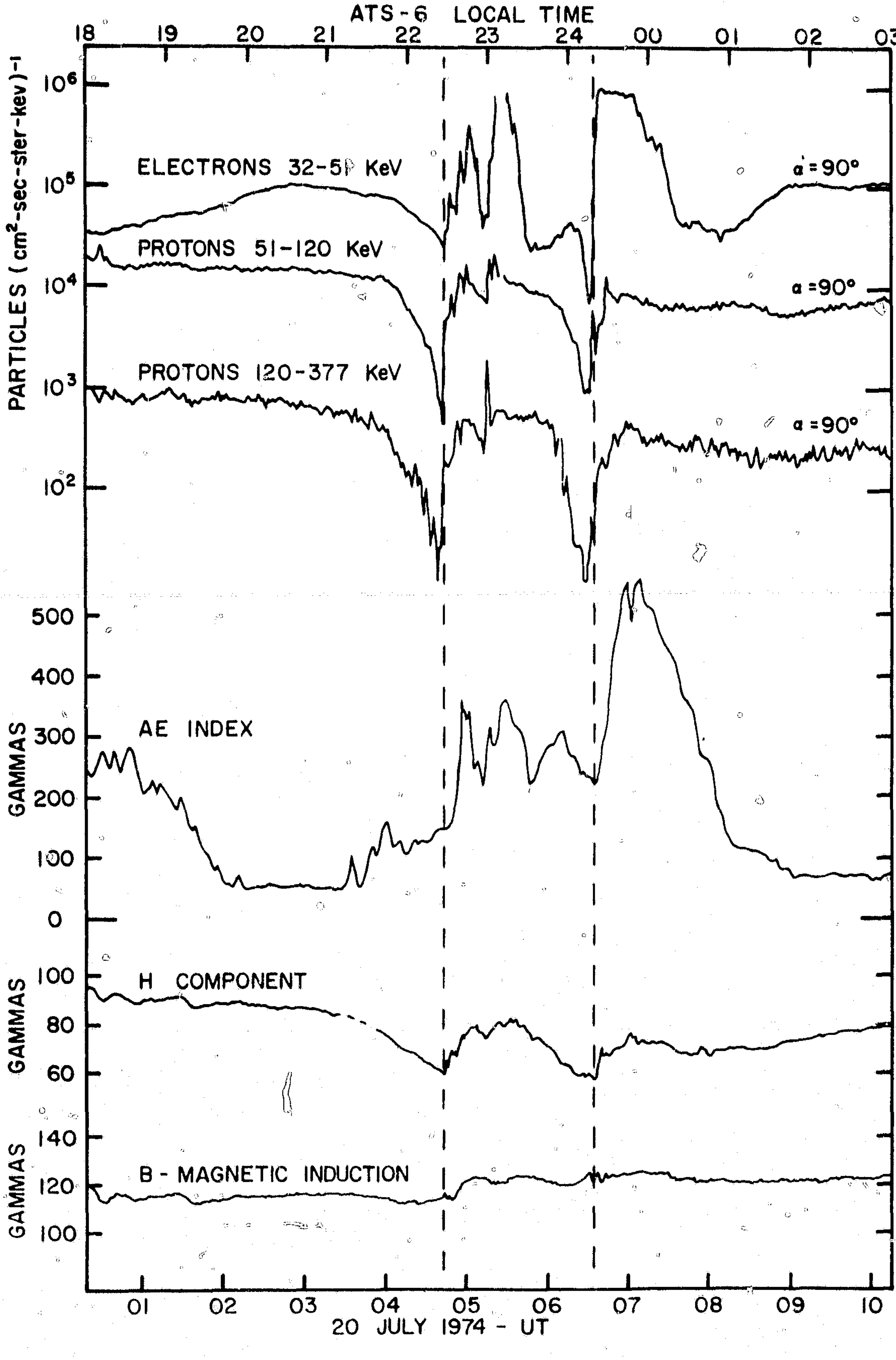
ATS-6 LOCAL TIME
18
19
20
21
22
23
24
00
01
02
03
PARTICLES (cm²-sec-ster-kev)⁻¹
10⁶
10⁵
10⁴
10³
10²
ELECTRONS 32-51 KeV
α = 90°
PROTONS 51-120 KeV
α = 90°
PROTONS 120-377 KeV
α = 90°
GAMMAS
500
400
300
200
100
0
AE INDEX
GAMMAS
100
80
60
H COMPONENT
GAMMAS
140
120
100
B - MAGNETIC INDUCTION
01
02
03
04
05
06
07
08
09
10
20 JULY 1974 - UT

FIGURE 3

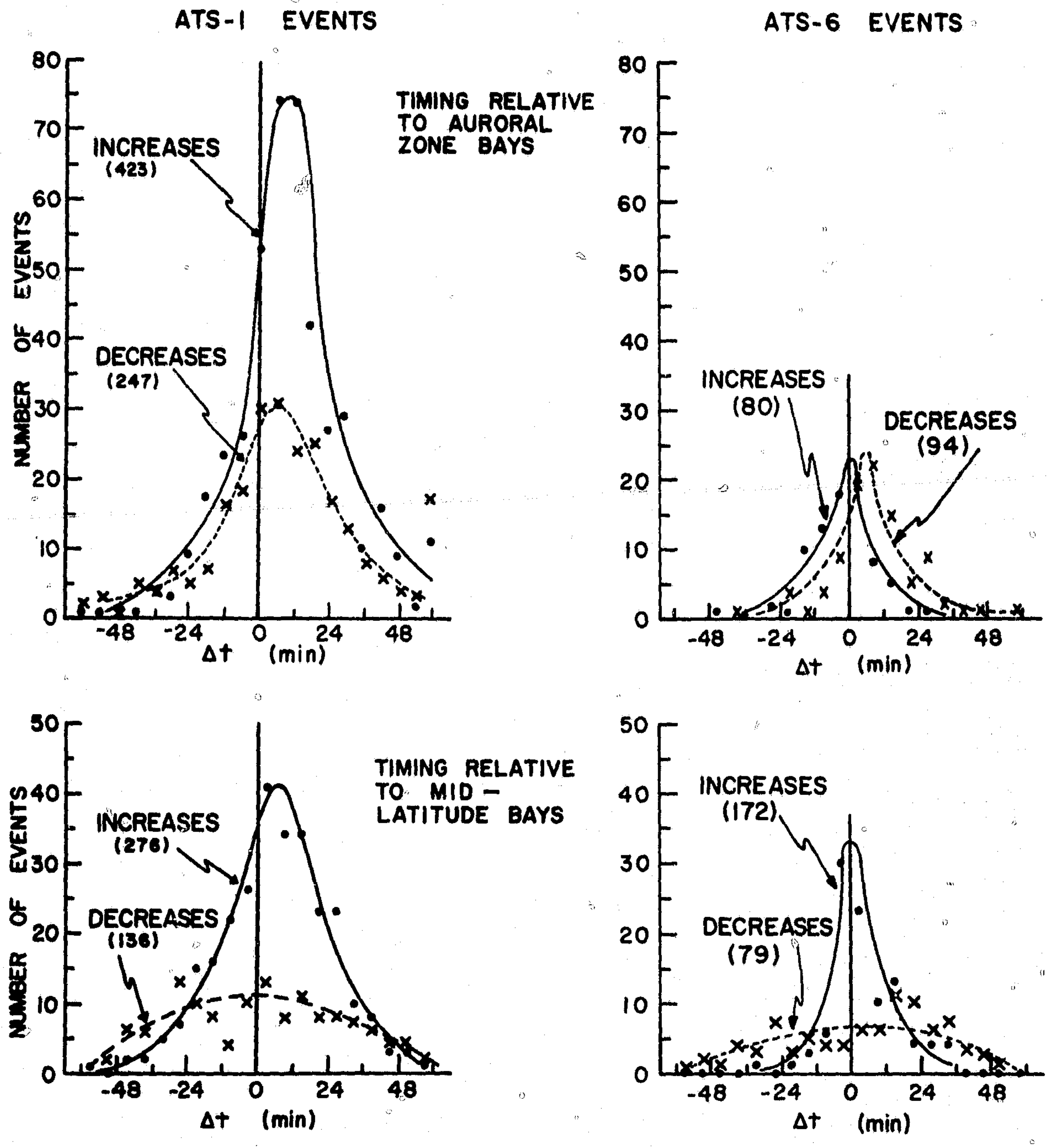
ATS-1 EVENTS
ATS-6 EVENTS
TIMING RELATIVE TO AURORAL ZONE BAYS
TIMING RELATIVE TO MID-LATITUDE BAYS
INCREASES (423)
DECREASES (247)
INCREASES (80)
DECREASES (94)
INCREASES (276)
DECREASES (136)
INCREASES (172)
DECREASES (79)
NUMBER OF EVENTS
Δt (min)

FIGURE 4

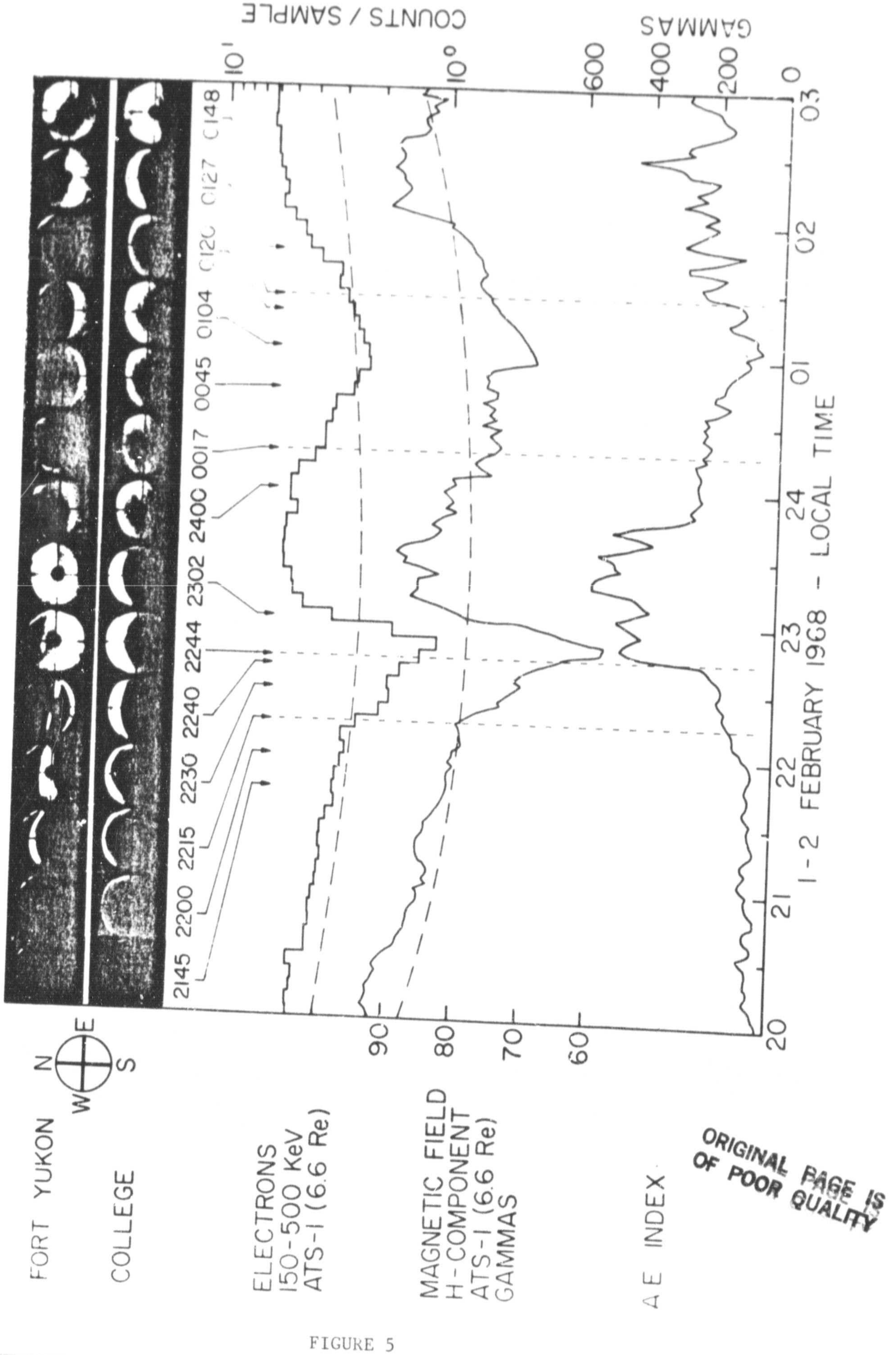
FORT YUKON
COLLEGE
N
E
S
W
ELECTRONS
150-500 KeV
ATS-1 (6.6 Re)
MAGNETIC FIELD
H-COMPONENT
ATS-1 (6.6 Re)
GAMMAS
AE INDEX
2145 2200 2215 2230 2240 2244 2302 2400 0017 0045 0104 0120 0127 0148
COUNTS / SAMPLE
10^1
10^0
90
80
70
60
GAMMAS
600
400
200
0
20 21 22 23 24 01 02 03
1-2 FEBRUARY 1968 - LOCAL TIME

FIGURE 5

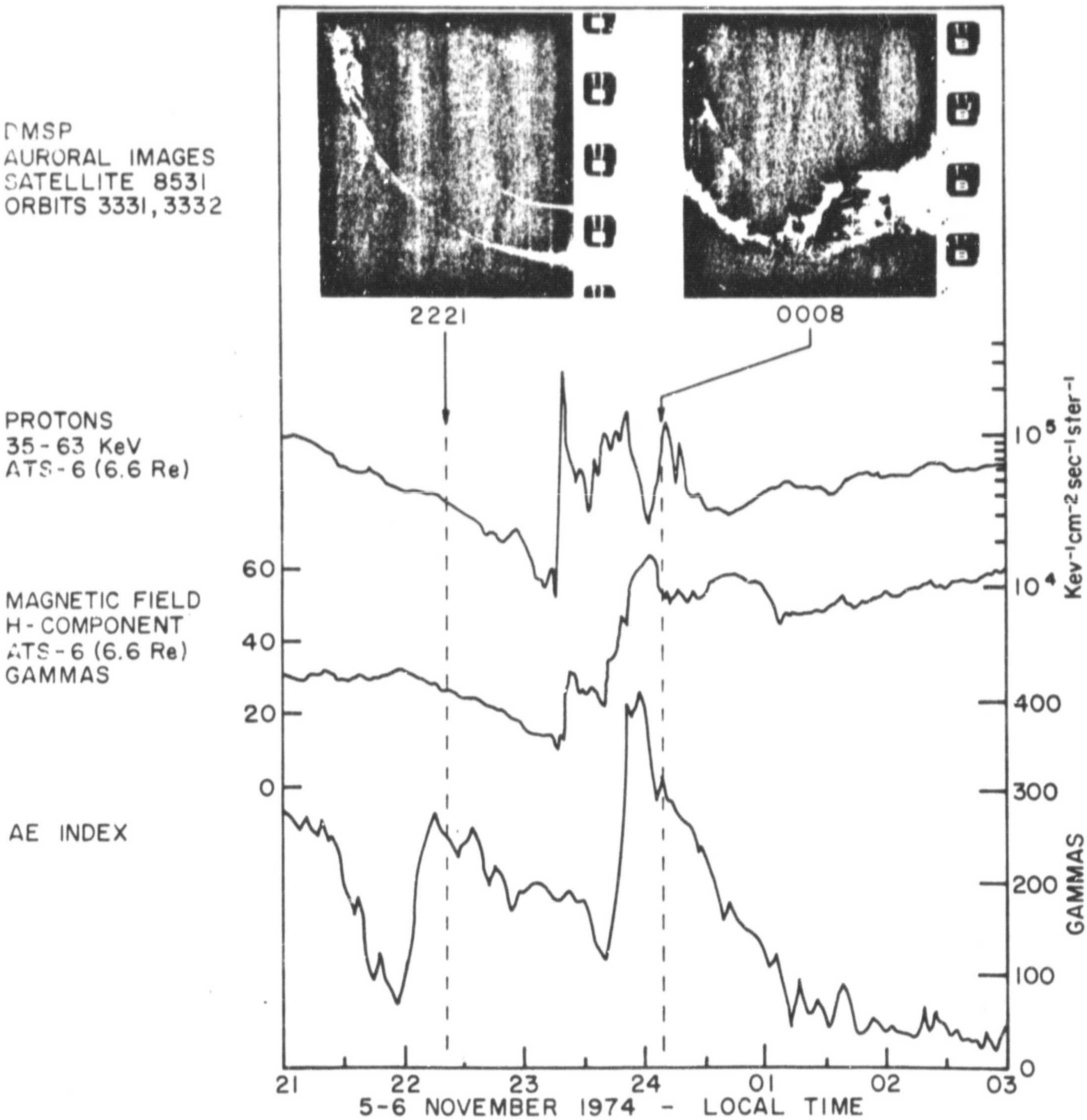
DMSP
AURORAL IMAGES
SATELLITE 8531
ORBITS 3331, 3332
2221
0008
PROTONS
35 - 63 KeV
ATS - 6 (6.6 Re)
MAGNETIC FIELD
H - COMPONENT
ATS - 6 (6.6 Re)
GAMMAS
60
40
20
0
AE INDEX
10^5
10^4
$Kev^{-1}cm^{-2}sec^{-1}ster^{-1}$
400
300
200
100
0
GAMMAS
21
22
23
24
01
02
03
5-6 NOVEMBER 1974 - LOCAL TIME

FIGURE 6

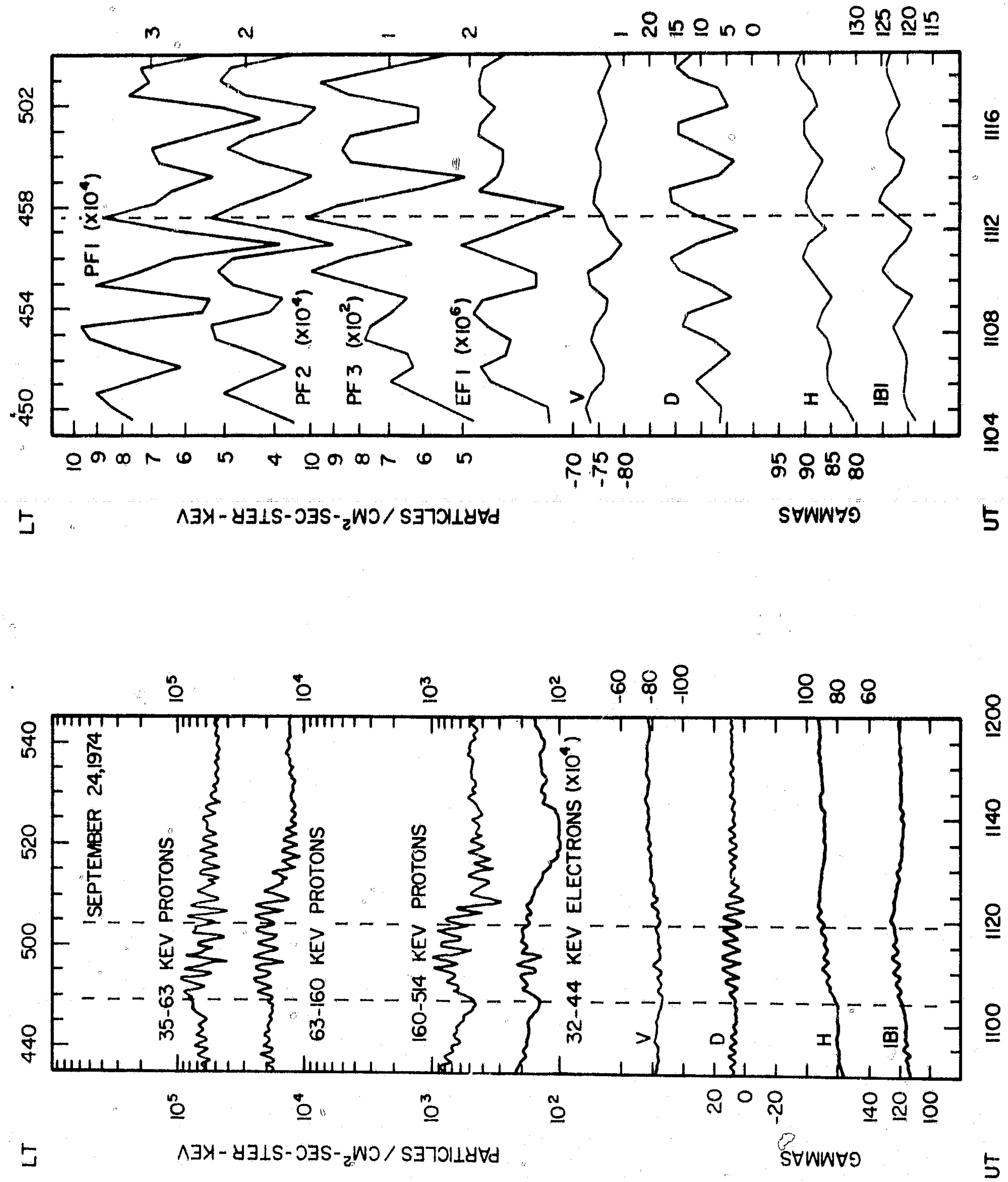
SEPTEMBER 24,1974
35-63 KEV PROTONS
63-160 KEV PROTONS
160-514 KEV PROTONS
32-44 KEV ELECTRONS (X10⁴)
V
D
H
IBI
PARTICLES / CM²-SEC-STER-KEV
GAMMAS
LT
UT
PF1 (X10⁴)
PF2 (X10⁴)
PF3 (X10²)
EF1 (X10⁶)

FIGURE 7

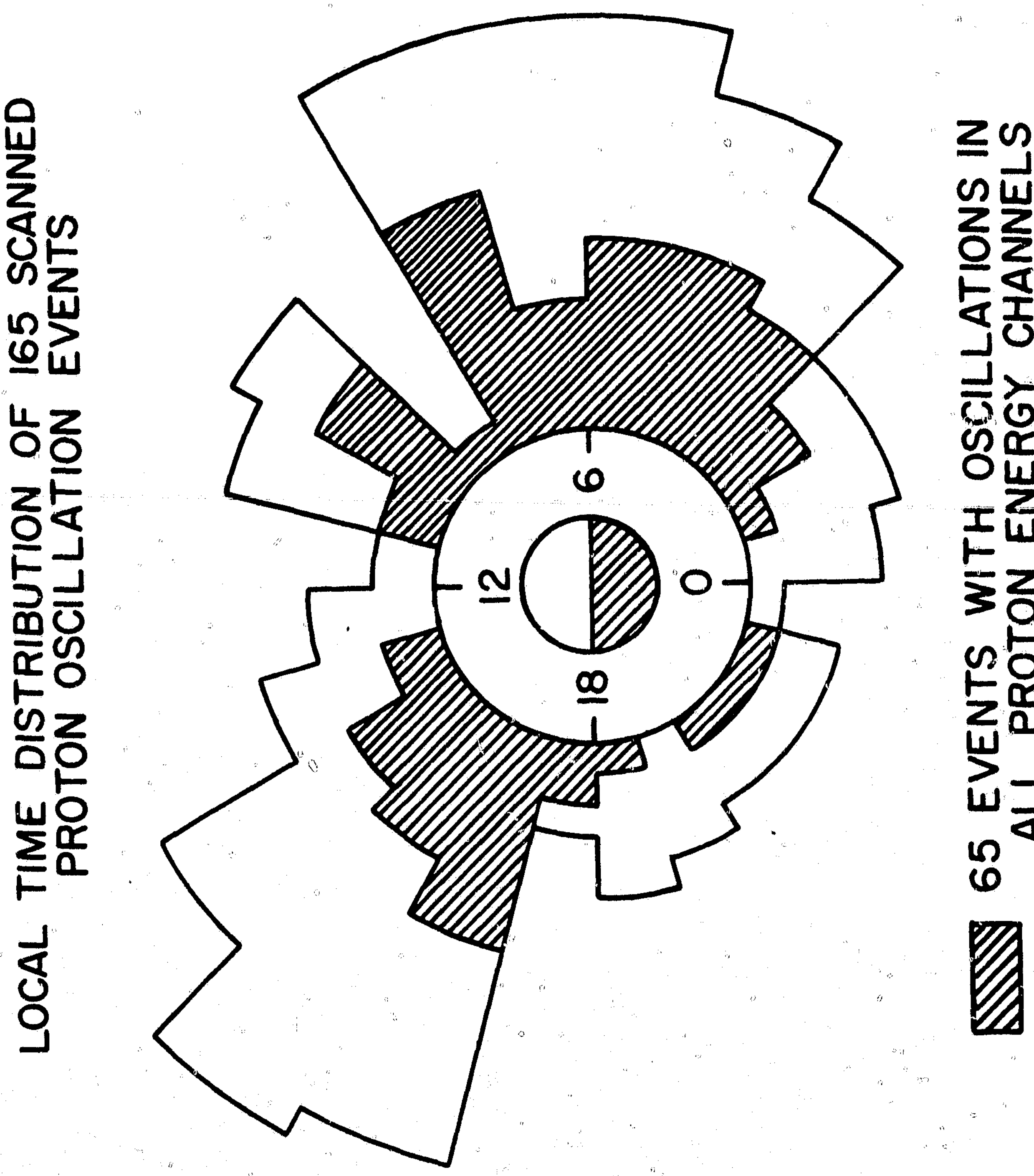
LOCAL TIME DISTRIBUTION OF 165 SCANNED PROTON OSCILLATION EVENTS
6
12
0
18
65 EVENTS WITH OSCILLATIONS IN ALL PROTON ENERGY CHANNELS

FIGURE 8